IMMUNOLOGY

Antiviral memory B cells exhibit enhanced innate immune response facilitated by epigenetic memory

Xiping Zhu[1,2]†, Sheng Hong[1]†, Jiachen Bu[1,2]†, Yingping Liu[1,3], Can Liu[3], Runhan Li[3], Tiantian Zhang[1,2], Zhuqiang Zhang[1,2], Liping Li[3,4], Xuyu Zhou[4,5], Zhaolin Hua[1,3]*, Bing Zhu[1,2,3,6]*, Baidong Hou[1,3]*

The long-lasting humoral immunity induced by viral infections or vaccinations depends on memory B cells with greatly increased affinity to viral antigens, which are evolved from germinal center (GC) responses. However, it is unclear whether antiviral memory B cells represent a distinct subset among the highly heterogeneous memory B cell population. Here, we examined memory B cells induced by a virus-mimicking antigen at both transcriptome and epigenetic levels and found unexpectedly that antiviral memory B cells exhibit an enhanced innate immune response, which appeared to be facilitated by the epigenetic memory that is established through the memory B cell development. In addition, T-bet is associated with the altered chromatin architecture and is required for the formation of the antiviral memory B cells. Thus, antiviral memory B cells are distinct from other GC-derived memory B cells in both physiological functions and epigenetic landmarks.

INTRODUCTION

Contagious diseases are still one of the main health issues in human societies. Memory B cells that are specific for viral antigens are critical for conferring long-term protection against recurrent viral infections and are examined to assess the population immunity and to evaluate vaccine efficacy (*1*). It is well appreciated that memory B cells in both mice and humans comprise a highly heterogeneous population with the expression of different surface molecules and functional diversity (*1*–*6*). For example, memory B cells expressing Ig-switched (swIg$^+$) B cell receptor (BCR) were found to differentiate more readily into plasma cells (PCs) than nonswitched IgM$^+$ memory B cells (*7*, *8*). However, it is also acknowledged that change of BCR alone, either by class switching or by somatic hypermutation (SHM), cannot fully account for the features of memory B cells (*9*–*12*). Changes in expression of surface markers, such as CD80 and PD-L2, have been shown to correlate with the differential potential of memory B cells more strongly than the BCR isotype (*13*, *14*). With the advance of more sophisticated multidimensional analysis, even more refined memory B cell subsets have been identified (*15*, *16*). Yet, the relationship between the phenotypic diversity of memory B cells and their in vivo physiological functions is largely unclear.

Curiously, although studies using model antigens demonstrated that memory B cells are generated more efficiently during the early germinal center (GC) response with low-affinity memory B cells as output (*17*–*19*), studies on various viral infections or vaccinations in humans have found that antiviral memory B cells, defined by antigen-specific binding, actually evolved over a long period (*20*–*29*). The SHM rate and the binding affinity to the antigen of these memory B cells gradually increased in several months after the clearance of initial infection, indicating that antiviral memory B cells are generated through a prolonged GC response. Given that antiviral memory B cells, exemplified by anti–smallpox vaccine–induced ones (*28*), can provide high-quality and long-lasting immune protection, knowing whether they are distinct from other GC-derived memory B cells and understanding how they are generated are critical for vaccine development.

To investigate the mechanism by which antiviral memory B cells are formed, we used bacterial phage Qβ-derived virus-like particle (Qβ-VLP) as a model antigen in mice. Qβ-VLP mimics viral structures in terms of both repetitive epitopes on the surface and encapsulated single-stranded RNA inside (*30*). B cell response induced by Qβ-VLP consequently mimics antiviral responses in many aspects. For example, it induces both T-independent and T-dependent antibody responses and a strong and prolonged GC response (*31*, *32*), and it activates Toll-like Receptor/Myeloid Differentiation Primary Response 88 (TLR/MyD88) signaling in antigen-specific B cells and drives a T helper 1 (T_H1)–oriented immune response (*33*–*36*). Moreover, the swIg$^+$ memory B cells induced by Qβ-VLP are stable for over a year in mice, and their BCRs are highly mutated and bind to antigens with increased affinity (*32*), like the antiviral memory B cells identified in humans. Because recent studies suggested that epigenetic differences underlie the heterogeneity of CD8$^+$ memory T cells (*37*, *38*) and epigenetic changes such as DNA methylation and chromatin remodeling have been observed in memory B cells (*39*–*41*), we explored changes of both transcriptome and chromatin accessibility at the different developmental stages of the memory B cells induced by Qβ-VLP. We also assessed the function of memory B cells by antigen re-challenge in vivo. We found unexpectedly that instead of a generally strengthened response, antiviral memory B cells exhibited an enhanced innate immune response upon re-challenge, which is associated with chromatin accessibility changes that are established in a stepwise manner from the early B cell activation to the GC B cell stage. Epigenetic memory likely contributes to the unique features of antiviral memory B cells. In addition, we identified T-bet as a main contributor to the generation of antiviral memory B cells, and

[1]Key Laboratory of Epigenetic Regulation and Intervention, Institute of Biophysics, Chinese Academy of Sciences, Beijing 100101, China. [2]National Laboratory of Biomacromolecules, Institute of Biophysics, Chinese Academy of Sciences, Beijing 100101, China. [3]College of Life Sciences, University of Chinese Academy of Sciences, Beijing 100049, China. [4]CAS Key Laboratory of Pathogenic Microbiology and Immunology, Institute of Microbiology, Chinese Academy of Sciences, Beijing, 100101, China. [5]Savaid Medical School, University of Chinese Academy of Sciences, Beijing, 100049, China. [6]New Cornerstone Science Laboratory, Institute of Biophysics, Chinese Academy of Sciences, Beijing 100101, China.
*Corresponding author. Email: zlhua@moon.ibp.ac.cn (Z.H.); zhubing@ibp.ac.cn (B.Z.); baidong_hou@ibp.ac.cn (B.H.)
†These authors contributed equally to this work.

specific chromatin accessible regions at the T-bet gene locus might serve as a marker for antiviral memory B cells.

RESULTS

Antiviral memory B cells evolve with progressive accumulation of SHMs and an increase of affinity

We previously showed that Qβ-VLP–induced GC response could last for 4 to 6 months in mice (*32*). Although IgM$^+$ memory B cells are induced at earlier time points after immunization, most Qβ-VLP–induced long-lasting memory B cells are swIg$^+$ (IgD$^-$IgM$^-$) (*32*) (Fig. 1A). This is consistent with what has been observed in humans that swIg$^+$ memory B cells are the ones that confer long-term protective immunity in antiviral responses (*2*). Thus, we focused on the swIg$^+$ memory B cells in this study and referred to them as "MemB" for simplicity. Qβ$^+$ MemB isolated from spleens exhibited similar characteristic surface markers as the swIg$^+$ memory B cells that have been identified under various other conditions not

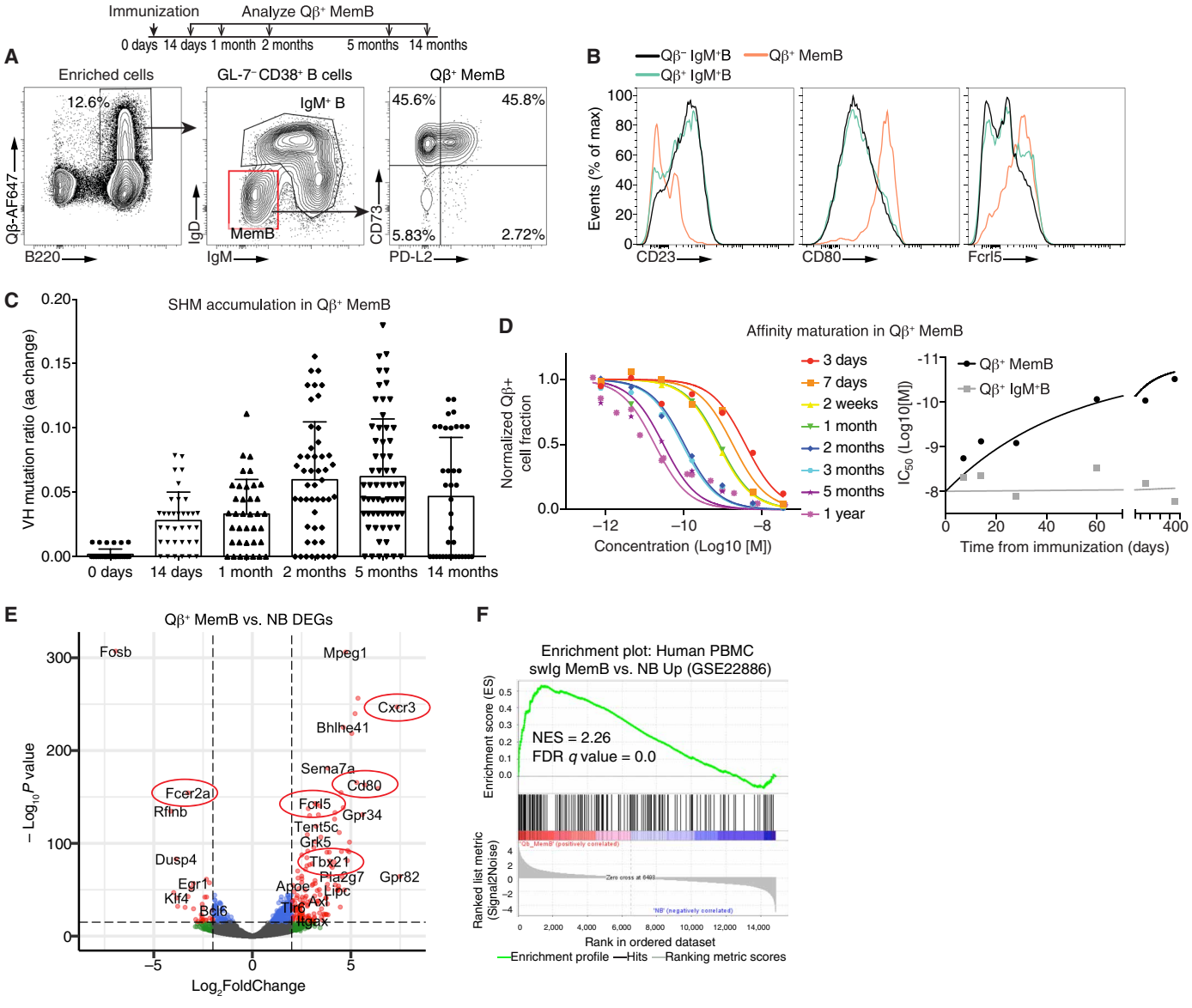

Fig. 1. Memory B cells induced by Qβ-VLP evolve with progressive accumulation of SHM and an increase in affinity. (**A**) Splenocytes were collected from mice immunized with Qβ-VLP at the indicated time points. Representative flow cytometry data from mice immunized 5 months previously show the gating strategy for Qβ$^+$ MemB and Qβ$^+$ IgM$^+$ B, along with the staining of CD73 and PD-L2 in Qβ$^+$ MemB. (**B**) Representative histograms show the down-regulation of CD23 and up-regulation of CD80 and Fcrl5 in Qβ$^+$ MemB at 5 months after immunization compared with naïve B cells. (**C**) Single Qβ$^+$ MemB sorted at the indicated time points underwent sequencing of the variable region of the heavy chain (VH). Mutations resulting in amino acid changes are quantified. (**D**) The affinity of Qβ$^+$ MemB to Qβ-VLP was measured by competitive inhibition at the indicated time points. The half-maximal inhibitory concentrations (IC_{50}) are plotted over time. (**E**) Qβ$^+$ MemB collected at 5 to 7 months after immunization underwent RNA-seq. Qβ$^+$ MemB versus NB DEGs are highlighted in the volcano plot based on expression change (|Log_2FoldChange| > 2) and statistical significance (–$Log_{10}P$ value >16). Genes of interest are circled. (**F**) GSEA showing the enrichment of human swIg$^+$ memory B cell–specific genes in Qβ$^+$ MemB versus NB DEGs (see also figs. S1 and S2).

necessarily relating to viral infections. These changes include up-regulation of CD73, PD-L2, and CD80 (Fig. 1, A and B, and fig. S1, A to C), which has been shown to correlate with stronger PC differential potential (*14*), and down-regulation of CD23 and CD62L, markers usually associated with naïve follicular B cells (fig. S1, C to E). Note that unlike what is reported for simple protein antigens, where most swIg$^+$ memory B cells are PD-L2$^+$ (*14*), only about half of Qβ$^+$ MemB are PD-L2$^+$ (Fig. 1A), suggesting a potential difference in the memory B cells induced by different types of antigens. Qβ$^+$ MemB also exhibited up-regulation of Fcrl5 (Fig. 1B and fig. S1C), which was originally identified on atypical memory B cells but shown recently to be also present on plasmodium-induced memory B cells (*42*), supporting that Fcrl5 is not an exclusive marker for atypical memory B cells. In contrast to Qβ$^+$ MemB, Qβ$^+$ IgM$^+$ B cells exhibited similar levels of the above-mentioned markers to Qβ$^-$ IgM$^+$ B cells (Fig. 1B and fig. S1, A and C to E), representing a heterogeneous population, with a large percentage likely being naïve B cells generated after the peak immune response. A small proportion of CD73$^+$PD-L2$^+$ cells within the Qβ$^+$ IgM$^+$ population, likely IgM$^+$ memory B cells, are not further investigated in this study.

We previously found that the number of Qβ$^+$ MemB peaked at 2 weeks after immunization and then gradually decreased and remained stable from 6 months to more than 1 year (*32*). The SHM ratio measured in Qβ$^+$ MemB cells continually increased from 2 weeks to 5 months after immunization (Fig. 1C), the period when Qβ$^+$ GC response is ongoing, suggesting that GC-derived memory B cells are continually replenishing the Qβ$^+$ MemB pool. Consistent with previous notions that GC B cells with relatively low affinity to antigen differentiate into memory B cells, we found that Qβ$^+$ MemB collected at early time points after immunization (before 2 weeks) were low-affinity, close to the level of Qβ$^+$ IgM$^+$ B cells. However, the affinity of Qβ$^+$ MemB gradually increased and reached near maximum at 5 months after immunization (Fig. 1D), suggesting that at least some of the initial low-affinity Qβ$^+$ MemB were replaced by the high-affinity memory B cells, which presumably are derived from the GC response. Together, our data provided an explanation to reconcile seemingly contradictory observations, i.e., most antiviral memory B cells are highly mutated and exhibit decent affinity to viral antigens while memory B cells are produced most efficiently number-wise at the beginning of an immune response from the low-affinity B cell pool. We propose that although low-affinity memory B cells dominate the early immune response, they can be partially replaced by the higher-affinity B cells derived from GC responses later. This process will be limited by the duration of the antigen-specific GC response, which is relatively short in the case of soluble protein immunizations but usually lasts much longer in antiviral or similar responses. Thus, Qβ$^+$ MemB, like other antiviral memory B cells, are derived from a prolonged GC response.

Alterations of chromatin accessibility in memory B cells reflect the gene activation history through B cell response

We focused our analysis on Qβ$^+$ MemB collected at 5 to 7 months after immunization, when the Qβ$^+$ MemB have become stable in cell number and mutation rate. To explore the potential characteristic change in antiviral memory B cells, we first analyzed the transcriptome of Qβ$^+$ MemB by RNA-seq. A number of differentially expressed genes (DEGs) in MemB versus naïve B cells (MemB versus NB) were identified, such as *Fcer2a* (CD23), *Cd80*, *Fcrl5*, *Cxcr3*, and *Tbx21* (Fig. 1E and table S1), many of which correlate well with changes in surface staining (Fig. 1B and fig. S1, C to E) and have been reported previously in relation to both murine and human memory B cells (*43*–*47*). Gene Set Enrichment Analysis (GSEA) also confirmed the evolutionary conservation between the swIg$^+$ human memory B cells and Qβ$^+$ MemB (Fig. 1F). Thus, Qβ$^+$ MemB are largely similar to previously identified swIg$^+$ memory B cells at the transcriptome level. Curiously, although the transcriptome of memory B cells is clearly distinguished from that of NB, it is unclear how memory B cells maintained their transcriptional network, as memory B cells lack any "master" TFs that could distinguish them from NB. We wondered whether epigenetic alterations might contribute to the transcriptional change in memory B cells. We then examined chromatin accessibility changes in Qβ$^+$ MemB compared with NB by Assay for Transposase-Accessible Chromatin using sequencing (ATAC-seq) and identified a large number of Qβ$^+$ MemB versus NB differentially accessible regions (DARs) (4416 open and 3700 closed) (fig. S2A). While most of the chromatin accessible regions are located outside the transcriptional start site (TSS) regions, the Qβ$^+$ MemB versus NB open DARs are further enriched in TSS-distal regions (fig. S2B), suggesting that MemB gained additional transcriptional regulatory elements during their differentiation.

We then examined the relationship between DARs and changes in gene expression. For genes associated with TSS-proximal DARs, their expression was largely correlated with the status of chromatin accessibility as expected; i.e., genes associated with open DARs were up-regulated and those associated with closed DARs were down-regulated (fig. S2C). These genes include *Cd80*, *Nt5e* (CD73), and *Sell* (CD62L), which are well-known for their characteristic changes in memory B cells (fig. S2D). However, because most of the DARs are not associated with gene promoters (fig. S2B), we extended our analysis to the complete set of Qβ$^+$ MemB versus NB DARs. Although the correlation between the DARs and gene expression changes appeared valid largely, there was a nearly equal fraction of DAR-associated genes showing no expression changes from NB to MemB (fig. S3A). We were curious about which genes they are and found that many of them are known to be involved in immune responses (table S2). To determine whether these genes are indeed involved in B cell responses, we examined the transcriptomes of B cells activated by Qβ-VLP in vivo at various stages (Fig. 2A and fig. S4), from the early antigen encounter (NB6h) to the later extrafollicular response at d3 (EFB and PCs), and then the GC response at d14 (GCB). Activation of most of the antigen-specific B cells at 6 hours after immunization was confirmed by the up-regulation of surface markers CD69 and CD83 (fig. S5B). We found that a large proportion of the Qβ$^+$ MemB versus NB open DAR-associated genes, although exhibiting no differences in gene expression between MemB and NB, had been up-regulated at various stages during the B cell response (fig. S3B). Many of these genes (clusters 3 and 4) were specifically up-regulated in the GCB stage (fig. S3B and table S2), such as *S1pr2*, a chemokine receptor involved in regulating GC homeostasis (*48*), and *Tox2*, a TF that has been shown to form a feed forward relationship with Bcl-6 in Tfh (*49*) (fig. S3C), consistent with the idea that the majority of Qβ-induced MemB are derived from GC response. A small fraction of these genes (cluster 5) were not up-regulated until the PC stage, such as *Ctla4*, a member of costimulatory molecules (*50*) (fig. S3, B and C), suggesting that Qβ$^+$ MemB might be primed to differentiate into PCs. Thus, Qβ$^+$ MemB versus NB DARs are associated with genes that are activated in previous cell stages, which Qβ$^+$ MemB presumably have passed through, suggesting that

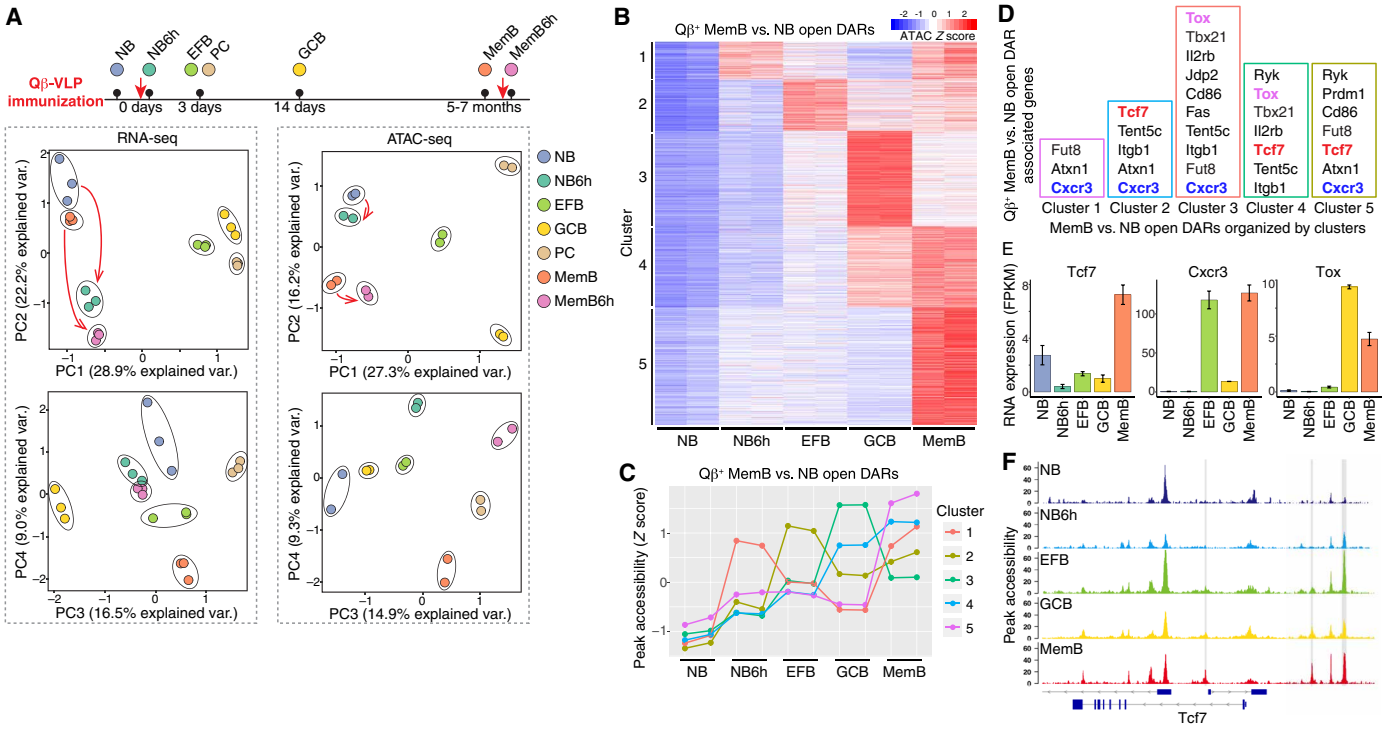

Fig. 2. Previous experiences of memory B cells are recorded as epigenetic memory. (**A**) NB and Qβ$^+$ B cell subsets collected at the indicated time points from mice immunized with Qβ-VLP once or twice underwent RNA-seq and ATAC-seq. PCA of RNA-seq and ATAC-seq data for the indicated cell groups are shown. (**B** to **F**) MemB versus NB open DARs are grouped by k-means clustering based on their accessibility at the indicated cell stages. Normalized peak reads (*Z* score) are shown in a heatmap (B) or as means of each cluster (C). (D) Examples of genes associated with one or multiple MemB versus NB DARs. Genes labeled in colors are further presented for their expression changes in (E). (F) *Tcf7* serves as an example demonstrating the progressive increases in chromatin accessibility in nearby regulatory regions. Gray stripes indicate MemB versus NB DARs (see also figs. S3 to S5).

the epigenetic alterations in Qβ$^+$ MemB may reflect the gene activation history during B cell responses.

To understand how the epigenetic status is established in memory B cells, we examined the chromatin accessibility by ATAC-seq in the earlier stages of Qβ$^+$ B cells (NB6h, EFB, and GCB) as well as in PC and MemB that encountered the antigen for a second time (MemB6h) (Fig. 2A). An initial principal components analysis (PCA) showed that the aforementioned cell groups are well separated at both transcriptome and chromatin accessibility levels (Fig. 2A), confirming the distinct identity of each cell group. While the antigen encounter induced marked changes in transcriptomes (NB to NB6h and MemB to MemB6h), the chromatin accessibilities changed relatively mildly (Fig. 2A). On the other hand, MemB and NB are more distinguished at the chromatin accessibility level than at the transcriptome level. This result suggested again that epigenetic alterations are not always directly correlated with transcriptional changes.

To test whether the epigenetic alterations in Qβ$^+$ MemB reflect the history of B cell activation, we examined the chromatin accessibility of the Qβ$^+$ MemB versus NB open DARs over the earlier stages of Qβ$^+$ B cells. Almost half of these regions (clusters 3 and 4) exhibited high levels of openness at the GC B cell stage (Fig. 2, B and C), suggesting a potential impact of the GC response on shaping the epigenetic landscape in memory B cells. The chromatin accessibility at the *S1pr2* and *Tox2* gene loci in MemB seemed to be the result of such an effect from the GC B cell stage (fig. S3D). Notably, a small fraction of Qβ$^+$ MemB versus NB open DARs gained prominent accessibility at the very beginning of the immune response (NB6h) or the extrafollicular response stage (EFB) (clusters 1 and 2) (Fig. 2, B and C), implying that earlier events in B cell activation might also contribute to the MemB epigenetic changes despite the dominant contribution from the GC B cell stage. Therefore, the epigenetic status of memory B cells might carry the footprints of their activation history.

We noticed that some genes, such as *Tcf7*, *Cxcr3*, and *Tox*, were associated with multiple Qβ$^+$ MemB versus NB DARs; the regions associated with these genes became open sequentially during B cell response (Fig. 2D). Expression of these genes might, however, be transient or delayed in some cases (Fig. 2E). *Tcf7*, encoding a TF critical for memory T cells (*37*), was not expressed until the MemB stage although several nearby chromatin regions had gained accessibility at earlier stages (Fig. 2, E and F). *Ctla4* with gained chromatin accessibility at the MemB stage was not expressed until the PC stage (fig. S3, C and D). This observation suggested that the epigenetic alterations in Qβ$^+$ MemB might not only be a passive consequence of the previous cell activation but also prepare the cells for their future destiny.

The epigenetic alterations prepared the Qβ$^+$ MemB for enhanced transcription of antiviral genes upon antigen re-encounter

To explore how epigenetic alterations may contribute to the memory B cell function, we examined the immediate response of Qβ$^+$ MemB upon antigen re-encounter (MemB6h) from both gene expression and chromatin accessibility aspects. First, the secondary response

(MemB6h versus MemB) seemed to be more robust than the primary response (NB6h versus NB) (Fig. 3A and fig. S6A), as one might expect. More genes were up-regulated (1383 > 923) or down-regulated (812 > 293) during the secondary response, and the chromatin accessibility appeared to be more dynamic during the secondary response as well. Comparing the DEG or DAR sets between the primary and the secondary responses, a large fraction of the up-regulated DEGs (707 genes) or open DARs (1298 peaks) from the primary response were also present in the secondary response (Fig. 3B), indicating that NB and MemB shared a substantial part of cell activation program. We then examined the DARs that are unique to the primary response and found interestingly that these DARs, either open (892 peaks) or closed (699 peaks), were maintained in the open or closed state in MemB at resting state and did not change further upon antigen reencounter (Fig. 3C and fig. S6D). The DEGs that are uniquely induced in the primary response (216 up-regulated and 221 down-regulated) exhibited similar patterns, in which the expression level of these genes in MemB was already set to the same level as in activated B cells (NB6h) (fig. S6C). Thus, it appeared that Qβ$^+$ MemB were poised to a state that is prepared for activation, consistent with the general notion that memory response is usually faster than the primary response.

Although it is generally assumed that the memory response is stronger than the primary response, more than two-thirds of the genes that were induced by Qβ-VLP in either the primary or the secondary response were up-regulated to comparable levels in both responses (cluster 1, 1159 genes) (Fig. 3D). The genes that indeed exhibited enhanced transcription in the secondary response (cluster 2, 440 genes) were specifically enriched for viral response genes, whereas the commonly up-regulated genes were mainly related to ribonucleoprotein functions (Fig. 3E). The selectivity of the gene subset toward the antiviral pathway suggested that the transcriptional enhancement induced in Qβ$^+$ MemB might not be a direct effect of increased BCR signaling. We then wondered whether epigenetic alterations in Qβ$^+$ MemB might contribute to the enhanced transcription. In support of this hypothesis, the enhanced induction of *Il6*, *Il27*, and *Cxcl10* (Fig. 3F), cytokines and chemokine known to be involved in antiviral responses, was accompanied by increased chromatin accessibility around these genes in quiescent MemB (Fig. 3G). Furthermore, among all the genes that showed enhanced transcription in the secondary response (cluster 2), about 30% was associated with increased chromatin accessibility in the resting MemB, whereas only 10% of the primary and secondary response shared genes (cluster 1) was associated with such kind of changes (Fig. 3H). Note that the up-regulation of these antiviral genes at the protein level may require additional regulation. For instance, TLR7 was induced to a similar extent at the protein level 6 hours after immunization in NB and MemB, while exhibiting a much higher level at the RNA level in MemB (fig. S6B).

Together, these results suggested that the epigenetic alterations in Qβ$^+$ MemB might contribute to the enhanced transcription of a selected group of genes in the secondary response.

The enhanced innate immune response in Qβ$^+$ MemB is determined by the nature of immunogens

Because the genes that exhibited transcriptional enhancement in the Qβ-VLP–induced secondary response are related to antiviral functions and Qβ-VLP is a virus-mimicking immunogen, we wondered whether the nature of antigens contributes to the selectiveness of this gene group. To test this hypothesis, we chose a different type of model antigen, the oligomeric protein phycoerythrin (PE), for immunization (*8*). We added CpG-containing oligonucleotides (CpG) in addition to alum as adjuvants to promote the class switch to IgG2b and IgG2a/c, trying to match the main isotypes induced by Qβ-VLP (Fig. 4A and fig. S7A). Most PE$^+$ swIg$^+$ memory B (PE$^+$ MemB) cells were IgG2b or IgG2a/c, although there was still a bias to IgG1 in PE$^+$ MemB compared with Qβ$^+$ MemB (Fig. 4B). By and large, PE$^+$ MemB and Qβ$^+$ MemB were very similar in transcriptome (fig. S8A), except for a small group of genes that were up-regulated to a greater extent in the Qβ$^+$ MemB (fig. S8, B and C, and table S3). Most memory B cell signature genes, such as CD73, CD80, PD-L2, and CD23, exhibited similar degrees of changes of expression in PE$^+$ MemB and Qβ$^+$ MemB compared with NB (Fig. 4C and fig. S7B).

We then examined the secondary response induced by PE. A large number of genes were up-regulated in the PE$^+$ MemB 6 hours after immunization (fig. S8D). Most PE-induced DEGs in the secondary response were also up-regulated or down-regulated in the Qβ-VLP–induced secondary response (Fig. 4D). A small subset of these genes exhibited enhanced transcription in the secondary response compared with the Qβ-VLP–induced primary response (Fig. 4E and fig. S8E), many of which are downstream of BCR signaling and involved in B cell activation, such as NFκB family genes, *Myc*, and *Irf4* (Fig. 4E). This result suggests that PE$^+$ MemB also acquired transcriptional memory, which might facilitate their response to the antigen. Although PE$^+$ MemB exhibited such a robust response, Qβ$^+$ MemB up-regulated many more genes (788 genes) upon antigen reencounter than PE$^+$ MemB did (Fig. 4D). Consistently, PCA of the transcriptomes also showed a greater distance at PC1 between MemB and MemB6h following Qβ-VLP immunization compared to PE immunization (Fig. 4F). Gene ontology (GO) analysis showed that the secondary response genes induced specifically by Qβ-VLP were enriched for viral response genes (Fig. 4G), suggesting that the enhanced transcription of antiviral genes indeed depends on the immunogen type. By excluding the overlapped DEGs from the Qβ-VLP–induced primary response and PE-induced secondary response, we found a group of genes (542) being uniquely up-regulated in the Qβ-VLP–induced secondary response (Fig. 4H and fig. S8F), many of which have been shown to be induced in innate immune responses, such as *Irf1* and *Irf7* induced by TLR signaling and *Oas* genes induced by interferon signaling (Fig. 4I). Therefore, although both PE$^+$ MemB and Qβ$^+$ MemB are IgG$^+$ memory B cells derived from GC response, the enhanced antiviral response is a unique feature of Qβ$^+$ MemB, which is highly likely to be caused by the virus-like nature of Qβ-VLP.

Antiviral memory B cells carry distinct marks of chromatin accessible regions at the T-bet gene locus

To explore the potential mechanisms underlying the unique feature of Qβ$^+$ MemB, we analyzed the predicted TF binding motifs from the ATACseq-identified chromatin accessible regions in Qβ$^+$ MemB. The motifs enriched from the global chromatin accessible regions were very similar between NB and Qβ$^+$ MemB. We then searched in the Qβ$^+$ MemB versus NB open DARs for the enriched TF motifs. Within either the newly formed peaks (1687 peaks) or the complete set of open DARs (4416 peaks), we consistently found Pit-Oct-Unc (POU), Nuclear Factor-kappa B (NFκB), Interferon Regulatory Factor (IRF), and T-box binding motifs being enriched (Fig. 5A and fig. S9, A and B). POU family TF *Pou2f2* (OCT2) plays a major role in establishing GC B cell chromatin status (*51*, *52*), and its main coactivator *Pou2f1*

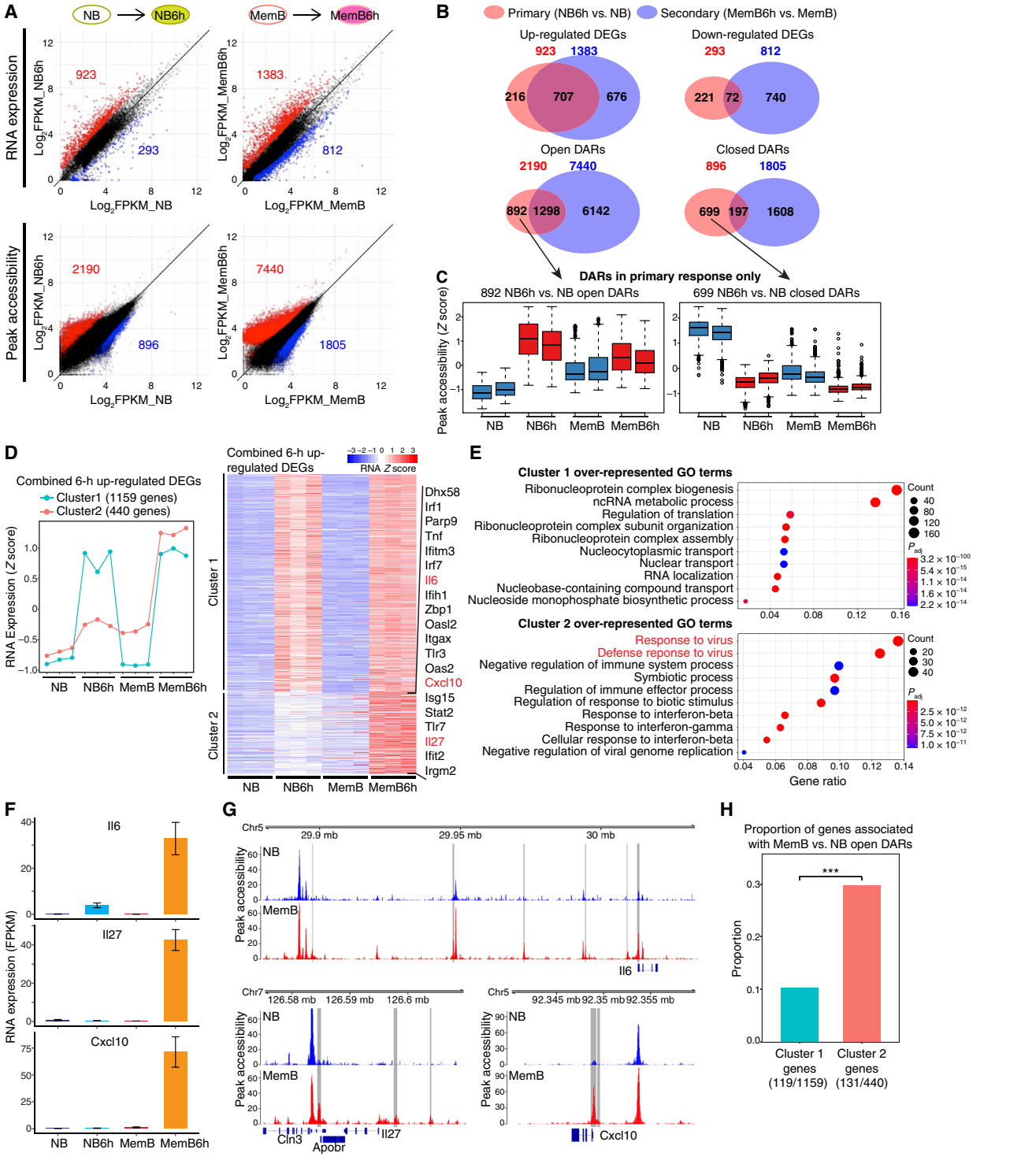

Fig. 3. Epigenetic alterations predispose Qβ$^+$ MemB to enhanced transcription of antiviral genes upon antigen re-challenge. (**A**) DEGs (|Log_2FoldChange| > 1) and DARs (|Log_2FoldChange| > 0.5) induced in primary (NB6h versus NB) and secondary (MemB6h versus MemB) responses to Qβ-VLP are highlighted in correlation plots of gene expression and peak accessibility (expressed as Log_2FPKM). (**B**) Venn diagrams show overlaps between the primary and secondary response-induced DEGs or DARs. (**C**) DARs specific to the primary response are analyzed for peak accessibility at the indicated cell stages, presented as boxplots of normalized reads. (**D**) Combined up-regulated DEGs from the primary and secondary responses are clustered into two groups by the k-means algorithm, with cluster 1 genes being commonly up-regulated in both primary and secondary responses and cluster 2 genes exhibiting enhanced transcription in the secondary response. Representative genes from cluster 2 are listed. (**E**) Top 10 over-represented GO terms of biological pathways from cluster 1 and cluster 2 genes. (**F** and **G**) Examples of cytokines and chemokines up-regulated in the secondary response to Qβ-VLP (F), with pre-existing chromatin accessibility changes in the quiescent Qβ$^+$ MemB (G). Gray stripes indicate MemB versus NB DARs. (**H**) The proportion of genes from cluster 1 or cluster 2 associated with MemB versus NB open DARs. Chi-square test was used for statistical analysis (***$P < 0.001$) (see also fig. S6).

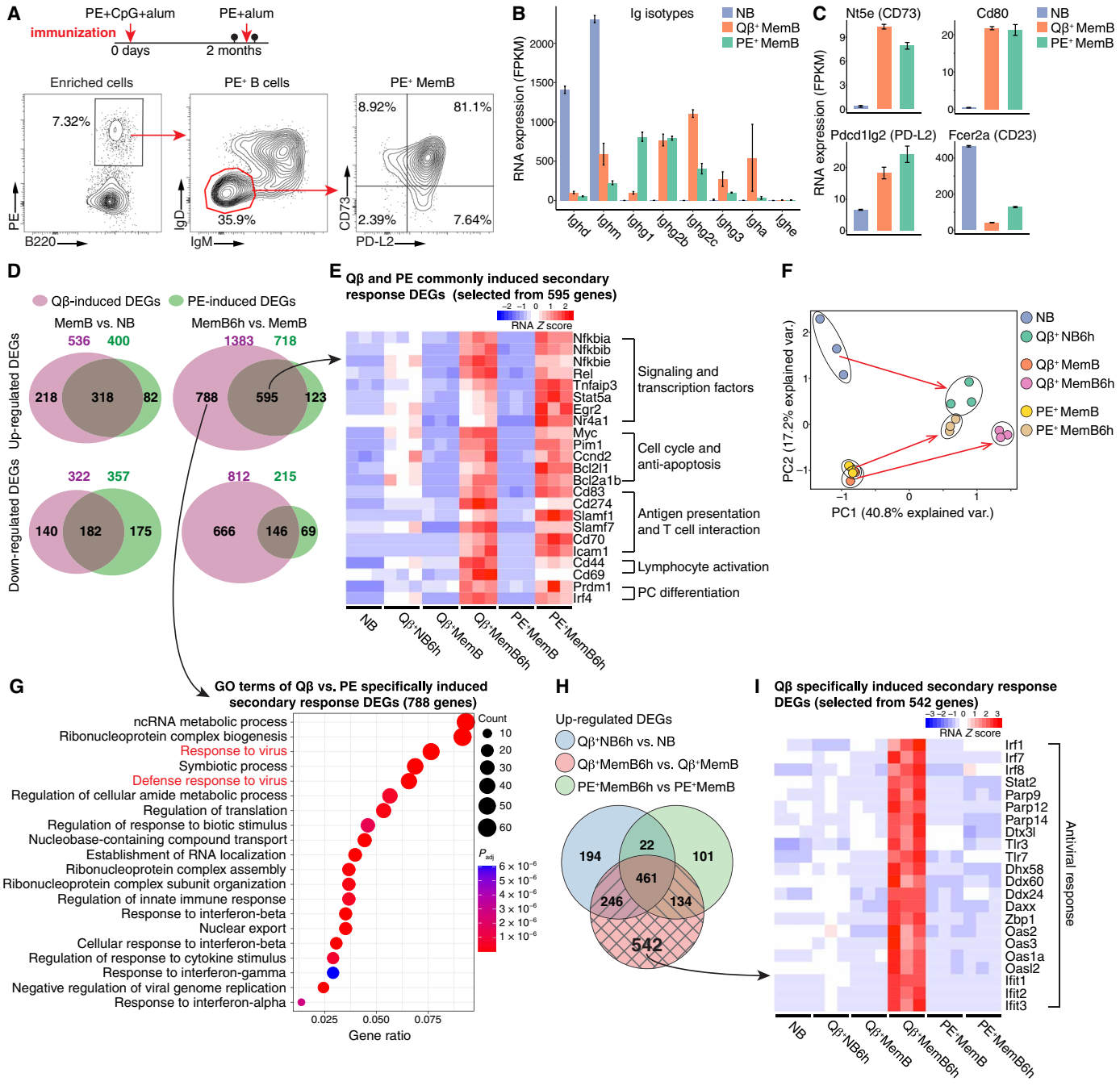

Fig. 4. The enhanced innate immune response in Qβ$^+$ MemB is determined by the nature of immunogens. (**A**) The diagram shows the regime for PE immunization. PE$^+$ MemB are gated as indicated, and the staining of CD73 and PD-L2 in PE$^+$ MemB is shown. (**B**) Expression levels of Ig isotypes and (**C**) common markers of memory B cells in Qβ$^+$ and PE$^+$ MemB. (**D**) Venn diagrams illustrate overlaps between MemB versus NB DEGs or MemB6h versus MemB DEGs induced by Qβ-VLP and PE. (**E**) Genes are selected from the overlapped MemB6h versus MemB DEGs [595 genes in (D)] induced by Qβ-VLP and PE, which exhibit enhanced transcription in the secondary responses compared with the Qβ-VLP–induced primary response (see also fig. S8E). (**F**) PCA of transcriptomes of the indicated cell groups. (**G**) Top 20 over-represented GO terms from Qβ-VLP versus PE specifically induced secondary response DEGs [788 genes in (D)]. (**H**) Venn diagram shows DEGs that are specific to the Qβ-VLP–induced secondary response. (**I**) Examples of genes from the 542 genes in (H) are shown for their expression levels (see also figs. S7 and S8).

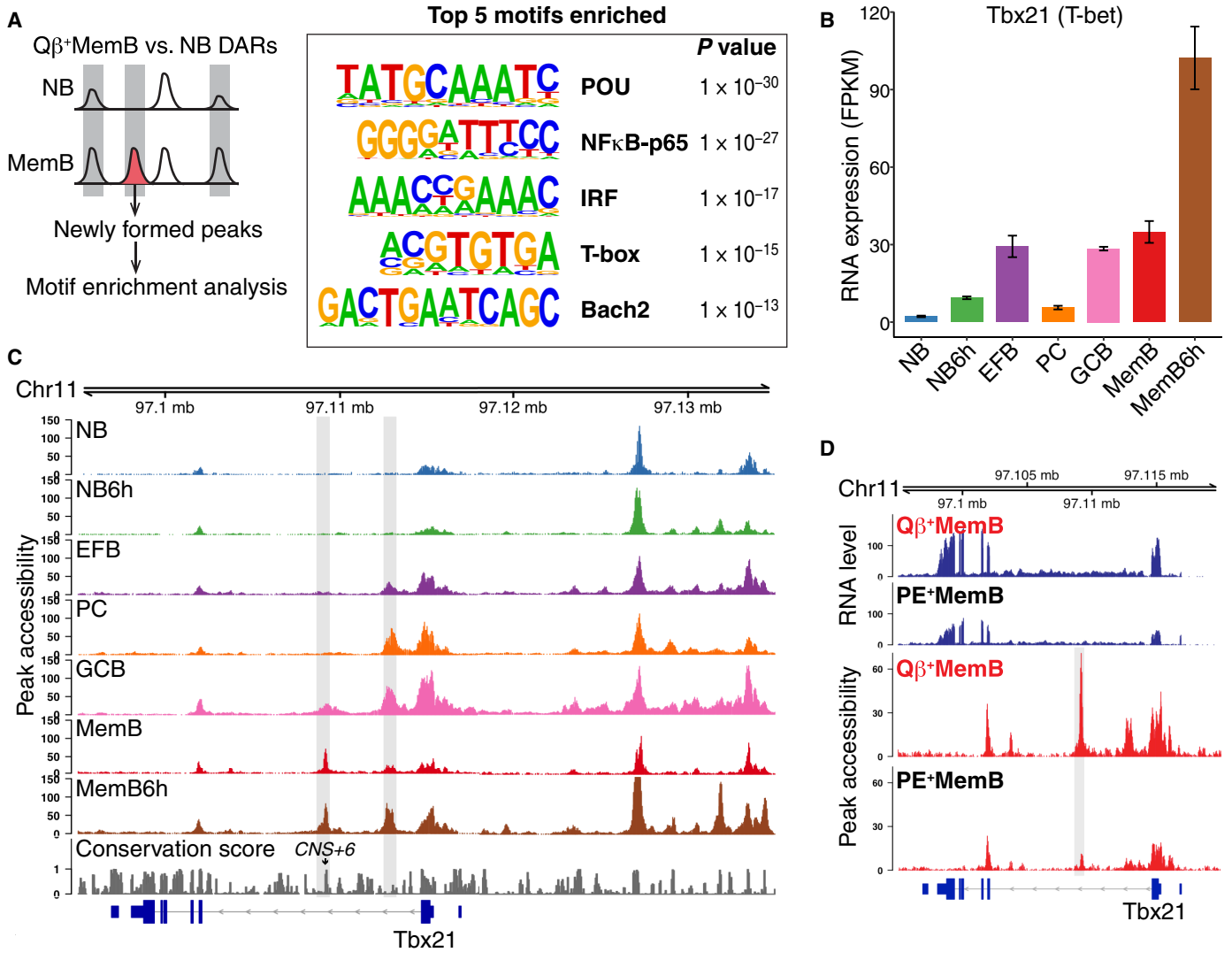

Fig. 5. T-bet is involved in maintaining the chromatin structures of Qβ$^+$ MemB. (**A**) Newly formed peaks from Qβ$^+$ MemB versus NB DARs were subjected to motif enrichment analysis. The top five statistically significant motifs are shown. (**B**) The expression level of T-bet at the indicated cell stages of Qβ$^+$ cells. (**C**) Progressive changes in chromatin accessibilities at the T-bet locus during the indicated cell stages. Gray stripes indicate Qβ$^+$ MemB versus NB DARs. The conserved noncoding sequence (*CNS*) at +6 kb from the T-bet promoter overlaps with one of the indicated DARs. (**D**) A comparison of chromatin accessibility at the Tbx21 locus between Qβ$^+$ MemB and PE$^+$ MemB (see also fig. S9).

(OCT1) was robustly up-regulated in GCB (fig. S9C). The enrichment of POU binding motifs in the Qβ$^+$ MemB likely reflected their GC origin. NFκB and IRF genes, on the other hand, were even slightly down-regulated in GCB and exhibited similar levels in NB and MemB (fig. S9C). NFκB and IRF TFs play important roles at multiple B cell stages, and they might be regulated posttranscriptionally or simply relocate to different chromatin regions during MemB formation.

The only TF whose expression correlates with the motif enrichment is T-box protein Tbx21 (T-bet), which was initially identified as the "master regulator" for T_H1 development and is also known to play important roles in the development and functional differentiation of a variety of adaptive and innate lymphocytes (*53*–*55*). The expression of T-bet during Qβ-induced B cell response was very dynamic (Fig. 5B). It was induced as early as 6 hours after immunization, then further increased in EFB, and maintained in GCB through MemB. Upon antigen re-encounter, T-bet was further up-regulated. The undulation of T-bet transcription at different cell stages suggested that T-bet itself might be subjected to epigenetic regulation. The chromatin accessibility at the T-bet gene locus was quite dynamic, showing distinct peak patterns at different cell stages even the RNA levels could sometimes be similar in these cells (Fig. 5C). Notably, Qβ$^+$ MemB gained two new accessible regions in the first intron of the T-bet gene compared with NB, one of which was acquired at the GCB stage and is also conserved evolutionarily (*CNS+6*, 6 kb downstream of TSS) (Fig. 5C). Moreover, PE$^+$ MemB, which expressed T-bet at a moderate level, lacked the *CNS+6* peak compared with Qβ$^+$ MemB (Fig. 5D and fig. S11A), suggesting that chromatin accessibility at the T-bet locus could be used to distinguish memory B cells raised against different types of immunogens. We cannot be certain whether T-bet contributes directly to the transcriptional program in

Qβ$^+$ MemB, although we found a small number of genes being upregulated in the Qβ$^+$ MemB, which are potential T-bet targets, such as *Zeb2*, *Cxcr3*, and *Igtax* (fig. S9D). Overall, it appeared that the alterations in epigenetic status might contribute to the permanent expression of T-bet in Qβ$^+$ MemB, and modifications at T-bet chromatin regions might be used to indicate the antiviral nature of memory B cells.

T-bet is required for the formation of Qβ$^+$ MemB

In B cells, T-bet is required for Ig class switching to IgG2a/c in mice (*56*), which is driven by TLR and interferon-γ (IFN-γ) signaling (*57*, *58*). T-bet also promotes PC formation in response to influenza infection (*59*, *60*). Despite the extensive studies of T-bet$^+$ B cells under different conditions, the role of T-bet in the generation or maintenance of memory B cells is controversial. It has been proposed that T-bet is specifically required for the formation of IgG2a/c$^+$ memory B cells (*61*). However, because T-bet is required for IgG2a/c class switching, a direct loss of IgG2a/c$^+$ memory B cells in the absence of T-bet could be explained by the class switching defect. Furthermore, an indirect loss of memory response indicated by the reduction of PC formation upon T-bet deletion could potentially be explained by the involvement of T-bet in promoting PC differentiation (*59*). To resolve whether T-bet is directly involved in memory B cell formation, we chose to use mixed bone marrow chimeric mice derived from WT and T-bet knockout (KO) mice so that the B cells with different genotypes would be exposed to the same environment and any effects caused by T-bet deficiency could be interpreted as a B cell–intrinsic effect. The mice were examined at 2–3 months after immunization when Qβ-VLP–induced GC response was still ongoing so that we could compare the different subsets of Qβ$^+$ cells simultaneously (Fig. 6A). T-bet deficiency caused a marked decrease in Qβ$^+$ MemB but did not affect Qβ$^+$ GCB (Fig. 6, A and C, and fig. S10, A and B). While the relative proportion of GCB seemed increased in the T-bet KO condition, the actual GCB cell numbers did not significantly differ from the WT condition (fig. S10B), indicating T-bet's primary role in promoting Qβ$^+$ MemB. We confirmed the expression of T-bet at the protein level in the WT Qβ$^+$ GCB and MemB (Fig. 6B and fig. S10, C and D). Thus, although both GCB and MemB expressed T-bet, only MemB were significantly reduced by the loss of T-bet. The remaining MemB in T-bet KO are CD73$^+$PD-L2$^+$ (fig. S10E). Furthermore, the Qβ$^+$ IgM$^+$ B cells, which contain both IgM$^+$ memory B cells and NB at this stage of the immune response, expressed T-bet at a moderate

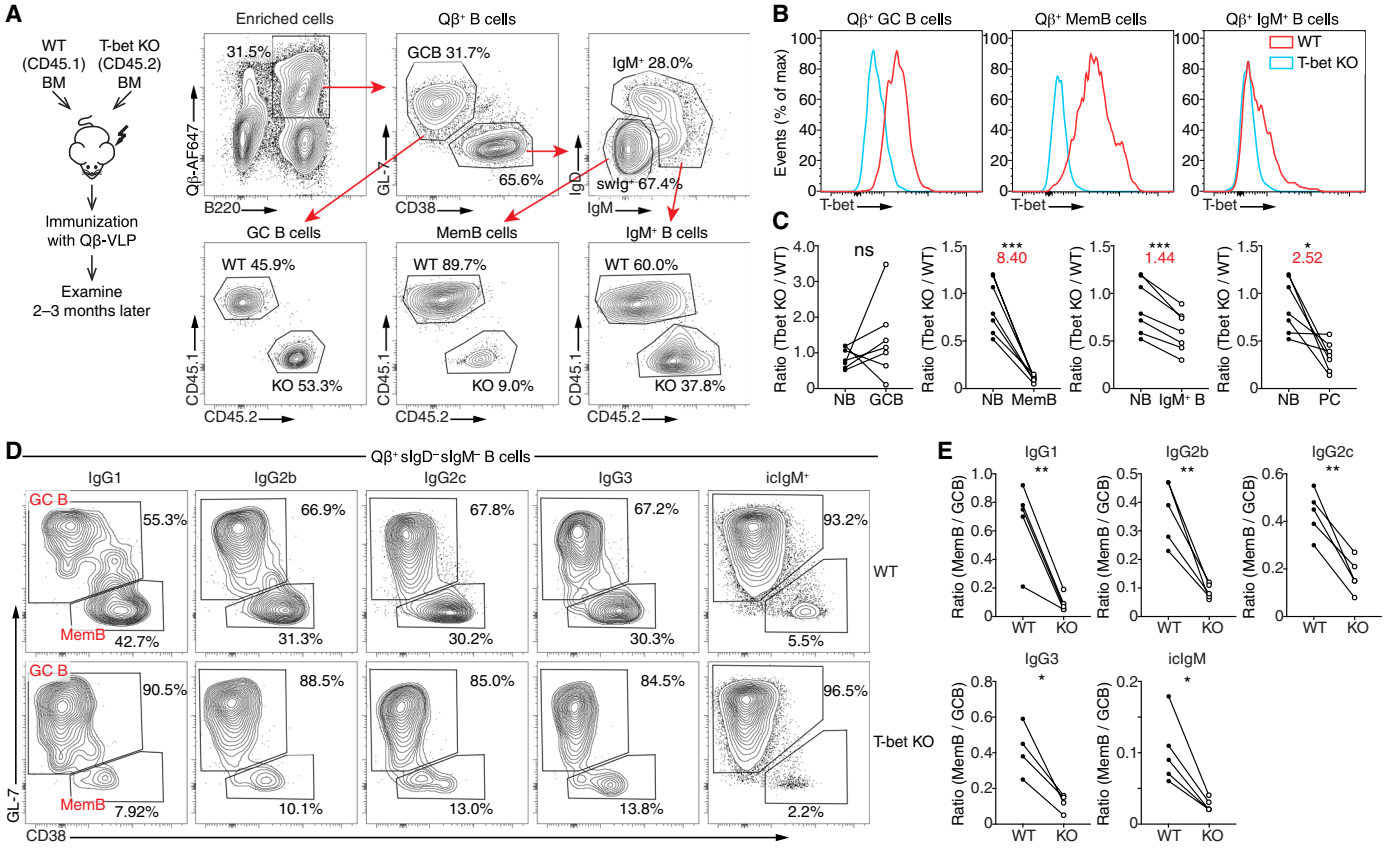

Fig. 6. T-bet is required for the formation of Qβ$^+$ MemB. (**A**) Bone marrow chimeric mice derived from WT and T-bet KO mice were immunized with Qβ-VLP and examined 2 to 3 months later. Representative flow cytometry data show the relative contribution of each donor to the indicated Qβ$^+$ cell groups. (**B**) Histogram of T-bet staining from the bone marrow chimeric mice as in (A). (**C**) Quantification of donor ratios for each indicated Qβ$^+$ cell group, as in (A). NB are total naïve B cells without gating for antigen specificity. The fold changes of the donor ratios from NB to the indicated Qβ$^+$ B cell groups are indicated in red letters. (**D**) Bone marrow chimeric mice were immunized and examined 2 to 3 weeks later. Surface IgD$^-$IgM$^-$ (sIgD$^-$IgM$^-$) cells gated from Qβ$^+$ B cells are further gated by different Ig isotypes as indicated. GL-7$^+$ GCB and CD38$^+$ MemB from each donor are then examined. (**E**) Quantification of MemB to GCB ratios for each isotype group as in (D). For (C) and (E), data from the same animal are connected by lines. A paired *t* test was used for statistical analysis (*P < 0.05, **P < 0.01, ***P < 0.001; ns, nonsignificant) (see also figs. S10 and S11).

level and were also slightly reduced in the T-bet KO-derived cells (Fig. 6, A and C), suggesting that the effect of T-bet on memory B cells is not limited to the class-switched ones.

Because T-bet deficiency led to a marked decrease in IgG2c$^+$ cells (*35*), we examined the MemB-to-GCB ratio for each Ig isotype in mice immunized 2 weeks previously to dissect the class-switch independent roles of T-bet. The Qβ$^+$ surface-IgD$^-$ IgM$^-$ (sIgD$^-$ sIgM$^-$) B cells included all the IgG subclasses and intracellular IgM (icIgM)–positive cells (Fig. 6D). Across all the Ig isotypes, T-bet KO showed a consistent reduction of MemB to GCB ratios (Fig. 6, D and E), suggesting that T-bet was required for the formation of Qβ$^+$ MemB independent of its function in class switching.

To investigate whether T-bet is uniquely required for the generation of antiviral memory B cells, we examined the formation of PE$^+$ MemB in the mixed bone marrow chimeric mice derived from WT and T-bet KO mice. PE$^+$ MemB also exhibited an increased level of T-bet compared to NB, but to a lesser degree compared with Qβ$^+$ MemB (fig. S11A). Accordingly, several predicted T-bet target genes, such as *Zeb2*, *Itgax*, and *Il2rb*, were expressed at lower levels in PE$^+$ MemB than in Qβ$^+$ MemB (fig. S11A). Consistent with the lower expression of T-bet in PE$^+$ MemB, there was a mild reduction of PE$^+$ MemB in T-bet KO donors (fig. S11, B to E). Therefore, T-bet was predominantly required for the memory B cells generated in antiviral-like responses.

Together, T-bet was required for the generation of viral response-induced memory B cells, regardless of their Ig isotypes. Because the Qβ$^+$ MemB was already largely reduced at the peak of GC response, the defect might occur in the transition from GCB to MemB, although a role of T-bet in maintaining the stability of memory B cells also needs to be explored in the future.

DISCUSSION

It is well acknowledged that memory B cells comprise a highly heterogeneous population. The cellular events B cells might go through, such as antigen encounter, activation of TLRs, interaction with T helper cells, and transition through GC B cell, might influence the features of the resulting memory B cells. In search for characteristics of antiviral memory B cells, we found unexpectedly that a subset of antiviral genes, most of which have been previously shown to be downstream of innate immune signaling, are selectively enhanced during the secondary response of Qβ$^+$ MemB. This phenomenon resembles innate memory, also known as trained immunity. Although innate immune memory has been observed under many different conditions and considered a more primitive but evolutionarily conserved form of memory (*62*), it is mostly identified in innate immune cells, such as natural killer cells, monocytes, and macrophages (*63*, *64*), and has not been considered much for the adaptive immune cells, i.e., T cells and B cells. The enhanced innate immune response in memory B cells could potentially be critical to ensure the proper memory response. Antiviral memory B cells, which express high-affinity BCRs for pathogens, could become targets of infection themselves. It has been shown that the influenza virus could infect naïve B cells expressing hemagglutinin-specific BCR derived from anti-influenza memory B cells through antigen receptors (*65*). However, most antiviral memory B cells are not depleted by repetitive viral infections. It is possible that the enhanced innate immune response protects the viral-specific memory B cells from being destructed. Furthermore, an enhanced ability to produce immune-modulating cytokines and chemokines could confer B cells additional effector functions beyond antibody secretion. For example, a recent study demonstrated that B cell–derived IL-27 is essential for controlling the chronic infection caused by lymphocytic choriomeningitis virus (*66*). Our data indicated that memory B cells are far more efficient in IL-27 production than naïve B cells. Yet, enhanced production of inflammatory cytokines by B cells might also contribute to pathological conditions. IL-6 by B cells has been implicated in the pathogenesis of autoimmunity (*67*). Further research is warranted to explore the potential contribution of memory B cells in these chronic conditions.

Here, we further demonstrated that epigenetic alterations might underlie the innate immune memory in B cells. A much higher proportion of the genes that are subjected to transcriptional enhancement in the secondary response is associated with increased chromatin accessibility in resting memory B cells (Fig. 3H), supporting the idea that epigenetic changes may prime these genes for expression. Although several recent studies reported similar transcriptome and chromatin accessibility changes in quiescent memory B cells as our study, they did not characterize the reactivation of memory B cells in detail (*40*, *68*). Because epigenetic machinery not only regulates gene expression at steady state but also determines cell response to external stimuli, it is important to challenge cells to fully reveal the physiological relevance of the epigenetic alterations. It is worth noting that a large fraction of Qβ$^+$ MemB versus NB DARs are associated with genes expressed specifically at the GCB stage. We are not certain whether these DARs confer any physiological functions or simply reflect the gene activation history. Nevertheless, we identified T-bet as a potential contributor to the epigenetic landscape of antiviral memory B cells because the T-bet binding motif is enriched in the Qβ$^+$ MemB versus NB DARs. The expression of the T-bet gene itself also seems to be subjected to epigenetic regulation, with a specific chromatin region at the T-bet gene locus turning accessible in Qβ$^+$ MemB but not in PE$^+$ MemB, suggesting that epigenetic marks may be used to distinguish different subsets of memory B cells.

Here, we also demonstrated that T-bet is required for the generation of Qβ$^+$ MemB. Although it may not be a surprise to find expression of T-bet in Qβ$^+$ MemB because T-bet$^+$ B cells have been found to associate with a variety of physiological and pathological conditions, including viral infections (*69*–*72*) and the development of lupus-like symptoms (*73*–*75*), it is unexpected to find that T-bet deficiency affected the formation of Qβ$^+$ MemB while leaving GCB largely intact. It has been shown in this study as well as by others (*55*, *76*) that T-bet could be expressed at various activation stages of a B cell, not limited to memory B cells. T-bet, as a TF, could promote class-switch and regulate gene expression in B cells. For example, T-bet may promote the expression of chemokine receptor *Cxcr3* to coordinate the migration of B cells to infectious sites (*77*), and T-bet level in B cells could contribute to their tissue distribution (*60*). However, within a small handful of potential T-bet target genes in Qβ$^+$ MemB, none is known to be essential for cell survival. Thus, the necessity of T-bet in the generation of Qβ$^+$ MemB could hardly be explained by its classical TF function. Another possibility is that T-bet could function as an epigenetic modifier, as exemplified in T_H1 development (*78*). It has also been demonstrated that differentiation of PCs driven by IFN-γ depends on T-bet to repress a group of genes (*59*), suggesting a more complicated role of T-bet in regulating cell differentiation. T-bet seems to promote PC generation in the secondary response upon influenza infection (*59*, *60*). The dependency on T-bet for the formation of antiviral memory B cells might ensure the availability of T-bet as a

critical TF during the secondary response. Our finding on the role of T-bet in generating antiviral memory B cells might also give a clue about why T-bet is often involved in chronic conditions, such as chronic infections or autoimmune diseases. A recent study reported that deficiency of T-bet in humans led to a decrease of a subset of memory B cells but left the humoral immunity largely intact (*79*), suggesting that other redundant mechanisms might be involved. Future studies are needed to understand the epigenetic role of T-bet in both mouse and human memory B cells.

In summary, we provide evidence supporting that epigenetic memory is established during the formation of memory B cells, which could contribute to an enhanced innate immune response in antiviral memory B cells. T-bet, potentially as an epigenetic regulator, is required for the formation of antiviral memory B cells.

MATERIALS AND METHODS

Animals

All experiments were approved by and carried out in accordance with guidelines of the Animal Care and Use Committee of the Institute of Biophysics (CAS, Beijing). All experimental mice were housed under specific pathogen–free (SPF) conditions. C57BL/6 were purchased from SPF (Beijing) Biotechnology Co. Ltd. or bred in-house. CD45.1 BoyJ (JAX 002014), *Tbx21*$^{-/-}$ (*80*) were originally from the sources listed in the references. Mixed bone marrow chimeric mice were generated by transplanting CD45.1 BoyJ and *Tbx21*$^{-/-}$ (at 1:1 ratio) mixed mouse BM cells into lethally irradiated (1000 rad) C57BL/6 mice. Littermates of the same sex at 8 to 12 weeks old or 8 weeks after transplantation were randomly assigned to experimental groups. Male and female mice were used in roughly equal numbers.

Immunization

Qβ-VLP (25 μg) in phosphate-buffered saline (PBS) or PE (25 μg) mixed with CpG (ODN1826, 50 μg) and alum was injected intraperitoneally.

Labeling and enrichment of antigen-specific B cells

Labeling and enrichment of Qβ-specific B cells (*32*) or PE-specific B cells (*8*) was done as previously described. In brief, Qβ-AF647 or PE was added to enzymatically dissociated splenocytes at 2 nM and incubated at 4 °C for 30 min. Cells were then incubated with anti-AF647 or anti-PE microbeads (Miltenyi Biotec) and isolated by magnetic column (Miltenyi Biotec). Qβ-GFP was added at 2 nM when it is necessary to distinguish Qβ$^+$ versus AF647$^+$ B cells.

Flow cytometry

Cells were suspended and stained in FACS (fluorescence-activated cell sorting) buffer (2% newborn calf serum, 2 mM EDTA, and 0.1%NaN_3 in PBS). For intracellular staining, cells were treated with Cytofix/Cytoperm solution (BD Biosciences) following the manufacturer's instruction. Antibody and reagents used for flow cytometry included the following: PE anti-T-bet (4B10), PE-CF594 anti-B220 (RA-6B2), APC-eF780 anti-B220 (RA3-6B2), PerCP-Cy5.5 anti-CD8 (53–6.7), PE-Cy7 anti-IgM (R6–60.2), FITC anti-IgM (R6–60.2), BV711 anti-IgD (11-26c.2a), PerCP-Cy5.5 anti-IgD (11-26c.2a), PE anti-GL-7 (GL-7), eF450 anti-GL-7 (GL-7), AF700 anti-CD38 (90), BV650 anti-CD19 (6D5), PE-Cy7 anti-CD19 (6D5), FITC anti-IgM (RMM-1), PE-Cy7 anti-IgM (1l/41), BV605 anti-CD73 (TY/11.8), PE anti-PD-L2 (TY25), FITC anti-CD45.1 (A20), Pacific Blue anti-CD45.1 (A20), APC-eF780 anti-CD45.2 (104), Pacific Blue anti-CD45.2 (104), PE-Cy7 streptavidin (BD Biosciences), and Pacific orange streptavidin (Invitrogen). All data were collected on a BD LSR Fortessa cytometer (BD) and analyzed with FlowJo (BD).

Mutation and affinity analysis

Mutation analysis was performed on single cells picked from sorted Qβ$^+$ MemB as described before (*32*). Population affinity of Qβ$^+$ MemB was measured by the competitive binding assay as described before (*32*).

Cell sorting

Naïve B (NB) cells were sorted from the splenocytes of the unimmunized mice as B220$^+$CD19$^+$IgD$^+$. For antigen-specific cells, Qβ-AF647$^+$ or PE$^+$ cells were first enriched from the splenocytes and then sorted. NB6h cells were collected 6 hours after immunization of naïve mice and sorted as B220$^+$CD19$^+$Qβ-AF647$^+$Qβ-GFP$^+$. Extrafollicularly activated B cells (EFB) and PCs were collected at day 3 after immunization as B220$^+$CD19$^+$Qβ-AF647$^+$Qβ-GFP$^+$ (EFB) and B220$^-$CD19$^-$Qβ-AF647$^+$ (PC). GC B cells were collected at day 14 after immunization as B220$^+$CD19$^+$Qβ-AF647$^+$CD38$^-$GL-7$^+$. FAS staining confirmed that all the GC B cells defined by these criteria were FAS^{hi} (fig. S5A). MemB were collected at 5 to 7 months after immunization of Qβ-VLP or 2 to 3 months after immunization of PE as Qβ-AF647$^+$ or PE$^+$ B220$^+$CD19$^+$ CD38$^+$GL-7$^-$IgD$^-$IgM$^-$. MemB6h cells were collected at 6 hours after the second immunization of previously immunized mice and sorted as Qβ-AF647$^+$ or PE$^+$ B220$^+$CD19$^+$ CD38$^+$GL-7$^-$IgD$^-$IgM$^-$. Samples were sorted with BD FACSAria III. Purities of 91.3 to 100% were yielded.

mRNA-seq

Total RNA from 5000 to 10,000 isolated mouse B cells were extracted by TRIzol Reagent (Life Technologies) and precipitated along with Glycogen (RNA grade) (Thermo Scientific). Then, mRNA was immediately isolated from total RNA with NEBNext Poly(A) mRNA Magnetic Isolation Module (E7490S). High-throughput sequencing libraries were constructed with NEBNext Ultra II RNA Library Prep Kit for Illumina (E7770S). Quality checking and sequencing were performed by Annoroad Gene Technology Co. Ltd. and BerryGenomics Co. Ltd. (Beijing, China). Illumina HiSeq X10 and Nova-Seq platforms with PE150 protocols were used for sequencing. Three biological replicates were sequenced for each cell group, with each biological replicate collected from one to two mice.

ATAC-seq

ATAC-seq was performed as previously described with some modifications (*81*). Basically, 10,000 cells from different stages were sorted by flow cytometry. Then, cells were washed once with ice-cold PBS and lysed with 50 μl of ice-cold lysis buffer (10 mM tris-HCl, pH 7.5, 10 mM NaCl, 3 mM $MgCl_2$, 0.1% NP-40, 0.1% Tween 20, and 0.01% digitonin) by incubating on ice for 10 min. The pellet was washed once with 1 ml of freshly prepared cold washing buffer (10 mM tris-HCl, pH 7.5, 10 mM NaCl, 3 mM $MgCl_2$, and 0.1% Tween 20). Transposition reaction was performed with TruePrep DNA Library Prep Kit V2 for Illumina kit (Vazyme, TD501) and incubated at 37 °C for 30 min on a thermomixer with shaking at 1,000 rpm. Finally, genome DNA was extracted with phenol-chloroform-isoamyl alcohol and amplified by KAPA HiFi HotStart ReadyMix (KAPA Biosystems,

KK2611) with barcoded primers (Vazyme, TD202). DNA fragments ranging from 200 to 1,000 bp were selected with VAHT DNA clean beads (Vazyme) for deep sequencing. Sequencing was performed using the same platforms as described for mRNA-seq. Two biological replicates were sequenced for each cell group, with each biological replicate collected from two mice.

RNA-seq and ATAC-seq analysis

Sequencing data were checked for quality using FastQC (v0.11.7) (*82*) and cleaned with Trimmomatic (v0.39) (*83*). The RNA-seq and ATAC-seq reads were mapped to the reference genome using HISAT2 (*84*). Mouse genome sequence GRCm38 and the annotation were downloaded from Ensembl archive release 97 (*85*). Mapped reads were then sorted and converted from .sam files to .bam files with Samtools (v1.9) (*86*). RNA fragment counts were obtained by counting paired-end reads containing exons using FeatureCounts (*87*). Fragments per kilobase of transcript per million mapped reads (FPKM) was calculated by a customized R script.

ATAC-seq peaks for each type of cells were called with Genrich (*88*) from the duplicated samples using the "ATAC-seq mode" with PCR duplicates removed, reads from mitochondrial and Y chromosome excluded, reads from a reference blacklist (*89*) removed, unpaired alignments kept, maximum q value as 0.05, and minimum AUC for a peak as 20.0. For comparing ATAC-seq peaks quantitatively, peaks from individual types of cells were merged by BEDTools (*90*) "unionbedg" and "merge" commands, and then reads located in the merged peak regions were counted with FeatureCounts (*87*). Deeptools (v3.2.1) (*91*) "bamCoverage" was used to convert genomic mapping results into bigwig format with "normalizeUsing RPKM'. Integrative genomics viewer (IGV) (v2.4.13) (*92*) was used to view the bigwig file. Motif enrichment from the ATAC-seq peaks was performed using HOMER (*93*, *94*) "findMotifsGenome.pl" command with defined background sequences. HOMER de novo motif results are presented. Genes associated with ATAC-seq peaks were defined as genes nearest to the peaks by HOMER "annotatePeaks.pl" command using the annotation database within HOMER program.

Statistical analysis

Differential analysis including DEGs and DARs was performed using DESeq2 (*95*) run as an R package. For the defined threshold of Log2FoldChange, apeglm (Approximate Posterior Estimation for generalized linear model) (*96*) was used for statistical analysis, and the s value <0.005 was considered to be statistically significant. For comparison without a defined threshold of Log2FoldChange, adjusted P value <0.1 was considered to be statistically significant. Genes expressing low levels (mean FPKM <1) are not included in further analysis.

PCA was performed in R using FPKM data in normalized mode, with genes expressing at low levels (mean FPKM <1) excluded. Graphs of PCA were generated using the R package "ggbiplot." Calculation of Z score was performed in R. Heatmap.2 in the R package "gplots" was used to generate the heatmap. K-means clustering was performed in R. Volcano plots were generated using the R package "EnhancedVolcano." The R package "Gviz" was used to generate sequencing plots of example genes. Venn diagrams were generated using the R package "VennDiagram." GO analysis and presentation were performed using the R package "clusterProfiler" (*97*). Gene-gene interaction was analyzed using STRING database on string-db.org (*98*). GSEA (*99*) was used to compare our data to the published human memory B cell data.

Paired Student's t test was used for statistical analysis in the mixed bone marrow chimeric mouse experiments.

Supplementary Materials

This PDF file includes:
Figs. S1 to S11
Legends for tables S1 to S3

Other Supplementary Material for this manuscript includes the following:
Tables S1 to S3

REFERENCES AND NOTES

1. D. Tarlinton, K. Good-Jacobson, Diversity among memory B cells: Origin, consequences, and utility. *Science* **341**, 1205–1211 (2013).
2. S. G. Tangye, D. M. Tarlinton, Memory B cells: Effectors of long-lived immune responses. *Eur. J. Immunol.* **39**, 2065–2075 (2009).
3. M. McHeyzer-Williams, S. Okitsu, N. Wang, L. McHeyzer-Williams, Molecular programming of B cell memory. *Nat. Rev. Immunol.* **12**, 24–34 (2011).
4. J. C. Weill, S. Le Gallou, Y. Hao, C. A. Reynaud, Multiple players in mouse B cell memory. *Curr. Opin. Immunol.* **25**, 334–338 (2013).
5. T. Kurosaki, K. Kometani, W. Ise, Memory B cells. *Nat. Rev. Immunol.* **15**, 149–159 (2015).
6. B. J. Laidlaw, J. G. Cyster, Transcriptional regulation of memory B cell differentiation. *Nat. Rev. Immunol.* **21**, 209–220 (2021).
7. I. Dogan, B. Bertocci, V. Vilmont, F. Delbos, J. Megret, S. Storck, C. A. Reynaud, J. C. Weill, Multiple layers of B cell memory with different effector functions. *Nat. Immunol.* **10**, 1292–1299 (2009).
8. K. A. Pape, J. J. Taylor, R. W. Maul, P. J. Gearhart, M. K. Jenkins, Different B cell populations mediate early and late memory during an endogenous immune response. *Science* **331**, 1203–1207 (2011).
9. T. Kaisho, F. Schwenk, K. Rajewsky, The roles of γ1 heavy chain membrane expression and cytoplasmic tail in IgG1 responses. *Science* **276**, 412–415 (1997).
10. S. W. Martin, C. C. Goodnow, Burst-enhancing role of the IgG membrane tail as a molecular determinant of memory. *Nat. Immunol.* **3**, 182–188 (2002).
11. K. L. Good, D. T. Avery, S. G. Tangye, Resting human memory B cells are intrinsically programmed for enhanced survival and responsiveness to diverse stimuli compared to naive B cells. *J. Immunol.* **182**, 890–901 (2009).
12. K. Kometani, R. Nakagawa, R. Shinnakasu, T. Kaji, A. Rybouchkin, S. Moriyama, K. Furukawa, H. Koseki, T. Takemori, T. Kurosaki, Repression of the transcription factor Bach2 contributes to predisposition of IgG1 memory B cells toward plasma cell differentiation. *Immunity* **39**, 136–147 (2013).
13. M. M. Tomayko, N. C. Steinel, S. M. Anderson, M. J. Shlomchik, Cutting edge: Hierarchy of maturity of murine memory B cell subsets. *J. Immunol.* **185**, 7146–7150 (2010).
14. G. V. Zuccarino-Catania, S. Sadanand, F. J. Weisel, M. M. Tomayko, H. Meng, S. H. Kleinstein, K. L. Good-Jacobson, M. J. Shlomchik, CD80 and PD-L2 define functionally distinct memory B cell subsets that are independent of antibody isotype. *Nat. Immunol.* **15**, 631–637 (2014).
15. D. R. Glass, A. G. Tsai, J. P. Oliveria, F. J. Hartmann, S. C. Kimmey, A. A. Calderon, L. Borges, M. C. Glass, L. E. Wagar, M. M. Davis, S. C. Bendall, An integrated multi-omic single-cell atlas of human B cell identity. *Immunity* **53**, 217–232.e5 (2020).
16. N. M. Weisel, S. M. Joachim, S. Smita, D. Callahan, R. A. Elsner, L. J. Conter, M. Chikina, D. L. Farber, F. J. Weisel, M. J. Shlomchik, Surface phenotypes of naive and memory B cells in mouse and human tissues. *Nat. Immunol.* **23**, 135–145 (2022).
17. F. J. Weisel, G. V. Zuccarino-Catania, M. Chikina, M. J. Shlomchik, A temporal switch in the germinal center determines differential output of memory B and plasma cells. *Immunity* **44**, 116–130 (2016).
18. R. Shinnakasu, T. Inoue, K. Kometani, S. Moriyama, Y. Adachi, M. Nakayama, Y. Takahashi, H. Fukuyama, T. Okada, T. Kurosaki, Regulated selection of germinal-center cells into the memory B cell compartment. *Nat. Immunol.* **17**, 861–869 (2016).
19. D. Suan, N. J. Krautler, J. L. V. Maag, D. Butt, K. Bourne, J. R. Hermes, D. T. Avery, C. Young, A. Statham, M. Elliott, M. E. Dinger, A. Basten, S. G. Tangye, R. Brink, CCR6 defines memory B cell precursors in mouse and human germinal centers, revealing light-zone location and predominant low antigen affinity. *Immunity* **47**, 1142–1153.e4 (2017).
20. S. F. Andrews, M. J. Chambers, C. A. Schramm, J. Plyler, J. E. Raab, M. Kanekiyo, R. A. Gillespie, A. Ransier, S. Darko, J. Hu, X. Chen, H. M. Yassine, J. C. Boyington, M. C. Crank, G. L. Chen, E. Coates, J. R. Mascola, D. C. Douek, B. S. Graham, J. E. Ledgerwood, A. B. McDermott, Activation dynamics and immunoglobulin evolution of pre-existing and newly generated human memory B cell responses to influenza hemagglutinin. *Immunity* **51**, 398–410.e5 (2019).

21. C. W. Davis, K. J. L. Jackson, A. K. McElroy, P. Halfmann, J. Huang, C. Chennareddy, A. E. Piper, Y. Leung, C. G. Albarino, I. Crozier, A. H. Ellebedy, J. Sidney, A. Sette, T. Yu, S. C. A. Nielsen, A. J. Goff, C. F. Spiropoulou, E. O. Saphire, G. Cavet, Y. Kawaoka, A. K. Mehta, P. J. Glass, S. D. Boyd, R. Ahmed, Longitudinal analysis of the human B cell response to ebola virus infection. *Cell* **177**, 1566–1582.e17 (2019).
22. A. Z. Wec, D. Haslwanter, Y. N. Abdiche, L. Shehata, N. Pedreno-Lopez, C. L. Moyer, Z. A. Bornholdt, A. Lilov, J. H. Nett, R. K. Jangra, M. Brown, D. I. Watkins, C. Ahlm, M. N. Forsell, F. A. Rey, G. Barba-Spaeth, K. Chandran, L. M. Walker, Longitudinal dynamics of the human B cell response to the yellow fever 17D vaccine. *Proc. Natl. Acad. Sci. U.S.A.* **117**, 6675–6685 (2020).
23. A. Sokal, G. Barba-Spaeth, I. Fernandez, M. Broketa, I. Azzaoui, A. de La Selle, A. Vandenberghe, S. Fourati, A. Roeser, A. Meola, M. Bouvier-Alias, E. Crickx, L. Languille, M. Michel, B. Godeau, S. Gallien, G. Melica, Y. Nguyen, V. Zarrouk, F. Canoui-Poitrine, F. Pirenne, J. Megret, J. M. Pawlotsky, S. Fillatreau, P. Bruhns, F. A. Rey, J. C. Weill, C. A. Reynaud, P. Chappert, M. Mahevas, mRNA vaccination of naive and COVID-19-recovered individuals elicits potent memory B cells that recognize SARS-CoV-2 variants. *Immunity* **54**, 2893, 2907.e5 (2021).
24. Z. Wang, F. Muecksch, D. Schaefer-Babajew, S. Finkin, C. Viant, C. Gaebler, H. H. Hoffmann, C. O. Barnes, M. Cipolla, V. Ramos, T. Y. Oliveira, A. Cho, F. Schmidt, J. Da Silva, E. Bednarski, L. Aguado, J. Yee, M. Daga, M. Turroja, K. G. Millard, M. Jankovic, A. Gazumyan, Z. Zhao, C. M. Rice, P. D. Bieniasz, M. Caskey, T. Hatziioannou, M. C. Nussenzweig, Naturally enhanced neutralizing breadth against SARS-CoV-2 one year after infection. *Nature* **595**, 426–431 (2021).
25. A. Sokal, P. Chappert, G. Barba-Spaeth, A. Roeser, S. Fourati, I. Azzaoui, A. Vandenberghe, I. Fernandez, A. Meola, M. Bouvier-Alias, E. Crickx, A. Beldi-Ferchiou, S. Hue, L. Languille, M. Michel, S. Baloul, F. Noizat-Pirenne, M. Luka, J. Megret, M. Menager, J. M. Pawlotsky, S. Fillatreau, F. A. Rey, J. C. Weill, C. A. Reynaud, M. Mahevas, Maturation and persistence of the anti-SARS-CoV-2 memory B cell response. *Cell* **184**, 1201–1213.e14 (2021).
26. C. Gaebler, Z. Wang, J. C. C. Lorenzi, F. Muecksch, S. Finkin, M. Tokuyama, A. Cho, M. Jankovic, D. Schaefer-Babajew, T. Y. Oliveira, M. Cipolla, C. Viant, C. O. Barnes, Y. Bram, G. Breton, T. Hagglof, P. Mendoza, A. Hurley, M. Turroja, K. Gordon, K. G. Millard, V. Ramos, F. Schmidt, Y. Weisblum, D. Jha, M. Tankelevich, G. Martinez-Delgado, J. Yee, R. Patel, J. Dizon, C. Unson-O'Brien, I. Shimeliovich, D. F. Robbiani, Z. Zhao, A. Gazumyan, R. E. Schwartz, T. Hatziioannou, P. J. Bjorkman, S. Mehandru, P. D. Bieniasz, M. Caskey, M. C. Nussenzweig, Evolution of antibody immunity to SARS-CoV-2. *Nature* **591**, 639–644 (2021).
27. R. R. Goel, M. M. Painter, S. A. Apostolidis, D. Mathew, W. Meng, A. M. Rosenfeld, K. A. Lundgreen, A. Reynaldi, D. S. Khoury, A. Pattekar, S. Gouma, L. Kuri-Cervantes, P. Hicks, S. Dysinger, A. Hicks, H. Sharma, S. Herring, S. Korte, A. E. Baxter, D. A. Oldridge, J. R. Giles, M. E. Weirick, C. M. McAllister, M. Awofolaju, N. Tanenbaum, E. M. Drapeau, J. Dougherty, S. Long, K. D'Andrea, J. T. Hamilton, M. McLaughlin, J. C. Williams, S. Adamski, O. Kuthuru; UPenn COVID Processing Unit, I. Frank, M. R. Betts, L. A. Vella, A. Grifoni, D. Weiskopf, A. Sette, S. E. Hensley, M. P. Davenport, P. Bates, E. T. L. Prak, A. R. Greenplate, E. J. Wherry, mRNA vaccines induce durable immune memory to SARS-CoV-2 and variants of concern. *Science* **374**, abm0829 (2021).
28. P. Chappert, F. Huetz, M. A. Espinasse, F. Chatonnet, L. Pannetier, L. Da Silva, C. Goetz, J. Megret, A. Sokal, E. Crickx, I. Nemazanyy, V. Jung, C. Guerrera, S. Storck, M. Mahevas, A. Cosma, P. Revy, T. Fest, C. A. Reynaud, J. C. Weill, Human anti-smallpox long-lived memory B cells are defined by dynamic interactions in the splenic niche and long-lasting germinal center imprinting. *Immunity* **55**, 1872–1890.e9 (2022).
29. W. Kim, J. Q. Zhou, S. C. Horvath, A. J. Schmitz, A. J. Sturtz, T. Lei, Z. Liu, E. Kalaidina, M. Thapa, W. B. Alsoussi, A. Haile, M. K. Klebert, T. Suessen, L. Parra-Rodriguez, P. A. Mudd, S. P. J. Whelan, W. D. Middleton, S. A. Teefey, I. Pusic, J. A. O'Halloran, R. M. Presti, J. S. Turner, A. H. Ellebedy, Germinal centre-driven maturation of B cell response to mRNA vaccination. *Nature* **604**, 141–145 (2022).
30. T. M. Kozlovska, I. Cielens, D. Dreilinna, A. Dislers, V. Baumanis, V. Ose, P. Pumpens, Recombinant RNA phage Q beta capsid particles synthesized and self-assembled in *Escherichia coli*. *Gene* **137**, 133–137 (1993).
31. D. Gatto, C. Ruedl, B. Odermatt, M. F. Bachmann, Rapid response of marginal zone B cells to viral particles. *J. Immunol.* **173**, 4308–4316 (2004).
32. W. Liao, Z. Hua, C. Liu, L. Lin, R. Chen, B. Hou, Characterization of T-dependent and T-independent B cell responses to a virus-like particle. *J. Immunol.* **198**, 3846–3856 (2017).
33. A. Jegerlehner, P. Maurer, J. Bessa, H. J. Hinton, M. Kopf, M. F. Bachmann, TLR9 signaling in B cells determines class switch recombination to IgG2a. *J. Immunol.* **178**, 2415–2420 (2007).
34. B. Hou, P. Saudan, G. Ott, M. L. Wheeler, M. Ji, L. Kuzmich, L. M. Lee, R. L. Coffman, M. F. Bachmann, A. L. DeFranco, Selective utilization of Toll-like receptor and MyD88 signaling in B cells for enhancement of the antiviral germinal center response. *Immunity* **34**, 375–384 (2011).
35. M. Tian, Z. Hua, S. Hong, Z. Zhang, C. Liu, L. Lin, J. Chen, W. Zhang, X. Zhou, F. Zhang, A. L. DeFranco, B. Hou, B cell-intrinsic MyD88 signaling promotes initial cell proliferation and differentiation to enhance the germinal center response to a virus-like particle. *J. Immunol.* **200**, 937–948 (2018).
36. S. Hong, Z. Zhang, H. Liu, M. Tian, X. Zhu, Z. Zhang, W. Wang, X. Zhou, F. Zhang, Q. Ge, B. Zhu, H. Tang, Z. Hua, B. Hou, B cells are the dominant antigen-presenting cells that activate naive $CD4^+$ T cells upon immunization with a virus-derived nanoparticle antigen. *Immunity* **49**, 695–708.e4 (2018).
37. Y. Chen, R. Zander, A. Khatun, D. M. Schauder, W. Cui, Transcriptional and epigenetic regulation of effector and memory CD8 T cell differentiation. *Front. Immunol.* **9**, 2826 (2018).
38. S. M. Gray, S. M. Kaech, M. M. Staron, The interface between transcriptional and epigenetic control of effector and memory $CD8^+$ T-cell differentiation. *Immunol. Rev.* **261**, 157–168 (2014).
39. A. Tsagaratou, C. J. Lio, X. Yue, A. Rao, TET methylcytosine oxidases in T cell and B cell development and function. *Front. Immunol.* **8**, 220 (2017).
40. J. B. Moroney, A. Vasudev, A. Pertsemlidis, H. Zan, P. Casali, Integrative transcriptome and chromatin landscape analysis reveals distinct epigenetic regulations in human memory B cells. *Nat. Commun.* **11**, 5435 (2020).
41. M. Zouali, DNA methylation signatures of autoimmune diseases in human B lymphocytes. *Clin. Immunol.* **222**, 108622 (2021).
42. C. C. Kim, A. M. Baccarella, A. Bayat, M. Pepper, M. F. Fontana, $FCRL5^+$ memory B cells exhibit robust recall responses. *Cell Rep.* **27**, 1446–1460.e4 (2019).
43. M. M. Tomayko, S. M. Anderson, C. E. Brayton, S. Sadanand, N. C. Steinel, T. W. Behrens, M. J. Shlomchik, Systematic comparison of gene expression between murine memory and naive B cells demonstrates that memory B cells have unique signaling capabilities. *J. Immunol.* **181**, 27–38 (2008).
44. D. Bhattacharya, M. T. Cheah, C. B. Franco, N. Hosen, C. L. Pin, W. C. Sha, I. L. Weissman, Transcriptional profiling of antigen-dependent murine B cell differentiation and memory formation. *J. Immunol.* **179**, 6808–6819 (2007).
45. A. R. Abbas, D. Baldwin, Y. Ma, W. Ouyang, A. Gurney, F. Martin, S. Fong, M. van Lookeren Campagne, P. Godowski, P. M. Williams, A. C. Chan, H. F. Clark, Immune response in silico (IRIS): Immune-specific genes identified from a compendium of microarray expression data. *Genes Immun.* **6**, 319–331 (2005).
46. A. A. Alizadeh, M. B. Eisen, R. E. Davis, C. Ma, I. S. Lossos, A. Rosenwald, J. C. Boldrick, H. Sabet, T. Tran, X. Yu, J. I. Powell, L. Yang, G. E. Marti, T. Moore, J. Hudson Jr., L. Lu, D. B. Lewis, R. Tibshirani, G. Sherlock, W. C. Chan, T. C. Greiner, D. D. Weisenburger, J. O. Armitage, R. Warnke, R. Levy, W. Wilson, M. R. Grever, J. C. Byrd, D. Botstein, P. O. Brown, L. M. Staudt, Distinct types of diffuse large B-cell lymphoma identified by gene expression profiling. *Nature* **403**, 503–511 (2000).
47. U. Klein, Y. Tu, G. A. Stolovitzky, J. L. Keller, J. Haddad Jr., V. Miljkovic, G. Cattoretti, A. Califano, R. Dalla-Favera, Transcriptional analysis of the B cell germinal center reaction. *Proc. Natl. Acad. Sci. U.S.A.* **100**, 2639–2644 (2003).
48. J. A. Green, K. Suzuki, B. Cho, L. D. Willison, D. Palmer, C. D. C. Allen, T. H. Schmidt, Y. Xu, R. L. Proia, S. R. Coughlin, J. G. Cyster, The sphingosine 1-phosphate receptor $S1P_2$ maintains the homeostasis of germinal center B cells and promotes niche confinement. *Nat. Immunol.* **12**, 672–680 (2011).
49. W. Xu, X. Zhao, X. Wang, H. Feng, M. Gou, W. Jin, X. Wang, X. Liu, C. Dong, The transcription factor Tox2 drives T follicular helper cell development via regulating chromatin accessibility. *Immunity* **51**, 826–839.e5 (2019).
50. C. A. Chambers, J. P. Allison, Costimulatory regulation of T cell function. *Curr. Opin. Cell Biol.* **11**, 203–210 (1999).
51. D. B. Schubart, A. Rolink, M. H. Kosco-Vilbois, F. Botteri, P. Matthias, B-cell-specific coactivator OBF-1/OCA-B/Bob1 required for immune response and germinal centre formation. *Nature* **383**, 538–542 (1996).
52. A. S. Doane, C. S. Chu, D. C. Di Giammartino, M. A. Rivas, J. C. Hellmuth, Y. Jiang, N. Yusufova, A. Alonso, R. G. Roeder, E. Apostolou, A. M. Melnick, O. Elemento, OCT2 pre-positioning facilitates cell fate transition and chromatin architecture changes in humoral immunity. *Nat. Immunol.* **22**, 1327–1340 (2021).
53. V. Lazarevic, L. H. Glimcher, G. M. Lord, T-bet: A bridge between innate and adaptive immunity. *Nat. Rev. Immunol.* **13**, 777–789 (2013).
54. A. Kallies, K. L. Good-Jacobson, Transcription factor T-bet orchestrates lineage development and function in the immune system. *Trends Immunol.* **38**, 287–297 (2017).
55. J. J. Knox, A. Myles, M. P. Cancro, $T\text{-bet}^+$ memory B cells: Generation, function, and fate. *Immunol. Rev.* **288**, 149–160 (2019).
56. S. L. Peng, S. J. Szabo, L. H. Glimcher, T-bet regulates IgG class switching and pathogenic autoantibody production. *Proc. Natl. Acad. Sci. U.S.A.* **99**, 5545–5550 (2002).
57. N. Liu, N. Ohnishi, L. Ni, S. Akira, K. B. Bacon, CpG directly induces T-bet expression and inhibits IgG1 and IgE switching in B cells. *Nat. Immunol.* **4**, 687–693 (2003).
58. K. Rubtsova, A. V. Rubtsov, L. F. van Dyk, J. W. Kappler, P. Marrack, T-box transcription factor T-bet, a key player in a unique type of B-cell activation essential for effective viral clearance. *Proc. Natl. Acad. Sci. U.S.A.* **110**, E3216–E3224 (2013).
59. S. L. Stone, J. N. Peel, C. D. Scharer, C. A. Risley, D. A. Chisolm, M. D. Schultz, B. Yu, A. Ballesteros-Tato, W. Wojciechowski, B. Mousseau, R. S. Misra, A. Hanidu, H. Jiang, Z. Qi,

J. M. Boss, T. D. Randall, S. R. Brodeur, A. W. Goldrath, A. S. Weinmann, A. F. Rosenberg, F. E. Lund, T-bet transcription factor promotes antibody-secreting cell differentiation by limiting the inflammatory effects of IFN-γ on B cells. *Immunity* **50**, 1172–1187.e7 (2019).
60. J. L. Johnson, R. L. Rosenthal, J. J. Knox, A. Myles, M. S. Naradikian, J. Madej, M. Kostiv, A. M. Rosenfeld, W. Meng, S. R. Christensen, S. E. Hensley, J. Yewdell, D. H. Canaday, J. Zhu, A. B. McDermott, Y. Dori, M. Itkin, E. J. Wherry, N. Pardi, D. Weissman, A. Naji, E. T. L. Prak, M. R. Betts, M. P. Cancro, The transcription factor T-bet resolves memory B cell subsets with distinct tissue distributions and antibody specificities in mice and humans. *Immunity* **52**, 842–855.e6 (2020).
61. N. S. Wang, L. J. McHeyzer-Williams, S. L. Okitsu, T. P. Burris, S. L. Reiner, M. G. McHeyzer-Williams, Divergent transcriptional programming of class-specific B cell memory by T-bet and RORα. *Nat. Immunol.* **13**, 604–611 (2012).
62. B. Gourbal, S. Pinaud, G. J. M. Beckers, J. W. M. Van Der Meer, U. Conrath, M. G. Netea, Innate immune memory: An evolutionary perspective. *Immunol. Rev.* **283**, 21–40 (2018).
63. C. M. Lau, G. M. Wiedemann, J. C. Sun, Epigenetic regulation of natural killer cell memory. *Immunol. Rev.* **305**, 90–110 (2022).
64. E. R. Sherwood, K. R. Burelbach, M. A. McBride, C. L. Stothers, A. M. Owen, A. Hernandez, N. K. Patil, D. L. Williams, J. K. Bohannon, Innate immune memory and the host response to infection. *J. Immunol.* **208**, 785–792 (2022).
65. S. K. Dougan, J. Ashour, R. A. Karssemeijer, M. W. Popp, A. M. Avalos, M. Barisa, A. F. Altenburg, J. R. Ingram, J. J. Cragnolini, C. Guo, F. W. Alt, R. Jaenisch, H. L. Ploegh, Antigen-specific B-cell receptor sensitizes B cells to infection by influenza virus. *Nature* **503**, 406–409 (2013).
66. I. Pratumchai, J. Zak, Z. Huang, B. Min, M. B. A. Oldstone, J. R. Teijaro, B cell-derived IL-27 promotes control of persistent LCMV infection. *Proc. Natl. Acad. Sci. U.S.A.* **119**, (2022).
67. T. Arkatkar, S. W. Du, H. M. Jacobs, E. M. Dam, B. Hou, J. H. Buckner, D. J. Rawlings, S. W. Jackson, B cell-derived IL-6 initiates spontaneous germinal center formation during systemic autoimmunity. *J. Exp. Med.* **214**, 3207–3217 (2017).
68. M. J. Price, C. D. Scharer, A. K. Kania, T. D. Randall, J. M. Boss, Conserved epigenetic programming and enhanced heme metabolism drive memory B cell reactivation. *J. Immunol.* **206**, 1493–1504 (2021).
69. L.-Y. Chang, Y. Li, D. E. Kaplan, Hepatitis C viraemia reversibly maintains subset of antigen-specific T-bet$^+$ tissue-like memory B cells. *J. Viral Hepat.* **24**, 389–396 (2017).
70. J. J. Knox, M. Buggert, L. Kardava, K. E. Seaton, M. A. Eller, D. H. Canaday, M. L. Robb, M. A. Ostrowski, S. G. Deeks, M. K. Slifka, G. D. Tomaras, S. Moir, M. A. Moody, M. R. Betts, T-bet$^+$ B cells are induced by human viral infections and dominate the HIV gp140 response. *JCI Insight* **2**, e92943 (2017).
71. N. Obeng-Adjei, S. Portugal, P. Holla, S. Li, H. Sohn, A. Ambegaonkar, J. Skinner, G. Bowyer, O. K. Doumbo, B. Traore, S. K. Pierce, P. D. Crompton, Malaria-induced interferon-γ drives the expansion of Tbethi atypical memory B cells. *PLOS Pathog.* **13**, e1006576 (2017).
72. B. E. Barnett, R. P. Staupe, P. M. Odorizzi, O. Palko, V. T. Tomov, A. E. Mahan, B. Gunn, D. Chen, M. A. Paley, G. Alter, S. L. Reiner, G. M. Lauer, J. R. Teijaro, E. J. Wherry, Cutting edge: B cell-intrinsic T-bet expression is required to control chronic viral infection. *J. Immunol.* **197**, 1017–1022 (2016).
73. A. V. Rubtsov, K. Rubtsova, A. Fischer, R. T. Meehan, J. Z. Gillis, J. W. Kappler, P. Marrack, Toll-like receptor 7 (TLR7)-driven accumulation of a novel CD11c$^+$ B-cell population is important for the development of autoimmunity. *Blood* **118**, 1305–1315 (2011).
74. Y. Hao, P. O'Neill, M. S. Naradikian, J. L. Scholz, M. P. Cancro, A B-cell subset uniquely responsive to innate stimuli accumulates in aged mice. *Blood* **118**, 1294–1304 (2011).
75. K. Rubtsova, A. V. Rubtsov, J. M. Thurman, J. M. Mennona, J. W. Kappler, P. Marrack, B cells expressing the transcription factor T-bet drive lupus-like autoimmunity. *J. Clin. Invest.* **127**, 1392–1404 (2017).
76. K. M. Nickerson, S. Smita, K. B. Hoehn, A. D. Marinov, K. B. Thomas, J. T. Kos, Y. Yang, S. I. Bastacky, C. T. Watson, S. H. Kleinstein, M. J. Shlomchik, Age-associated B cells are heterogeneous and dynamic drivers of autoimmunity in mice. *J. Exp. Med.* **220**, (2023).
77. A. Mendoza, W. T. Yewdell, B. Hoyos, M. Schizas, R. Bou-Puerto, A. J. Michaels, C. C. Brown, J. Chaudhuri, A. Y. Rudensky, Assembly of a spatial circuit of T-bet-expressing T and B lymphocytes is required for antiviral humoral immunity. *Sci. Immunol.* **6**, eabi4710 (2021).
78. S. A. Miller, A. S. Weinmann, Molecular mechanisms by which T-bet regulates T-helper cell commitment. *Immunol. Rev.* **238**, 233–246 (2010).
79. R. Yang, D. T. Avery, K. J. L. Jackson, M. Ogishi, I. Benhsaien, L. Du, X. Ye, J. Han, J. Rosain, J. N. Peel, M. A. Alyanakian, B. Neven, S. Winter, A. Puel, B. Boisson, K. J. Payne, M. Wong, A. J. Russell, Y. Mizoguchi, S. Okada, G. Uzel, C. C. Goodnow, S. Latour, J. El Bakkouri, A. Bousfiha, K. Preece, P. E. Gray, B. Keller, K. Warnatz, S. Boisson-Dupuis, L. Abel, Q. Pan-Hammarstrom, J. Bustamante, C. S. Ma, J. L. Casanova, S. G. Tangye, Human T-bet governs the generation of a distinct subset of CD11c^{high}CD21^{low} B cells. *Sci. Immunol.* **7**, eabq3277 (2022).
80. S. J. Szabo, B. M. Sullivan, C. Stemmann, A. R. Satoskar, B. P. Sleckman, L. H. Glimcher, Distinct effects of T-bet in T_H1 lineage commitment and IFN-γ production in CD4 and CD8 T cells. *Science* **295**, 338–342 (2002).
81. M. R. Corces, A. E. Trevino, E. G. Hamilton, P. G. Greenside, N. A. Sinnott-Armstrong, S. Vesuna, A. T. Satpathy, A. J. Rubin, K. S. Montine, B. Wu, A. Kathiria, S. W. Cho, M. R. Mumbach, A. C. Carter, M. Kasowski, L. A. Orloff, V. I. Risca, A. Kundaje, P. A. Khavari, T. J. Montine, W. J. Greenleaf, H. Y. Chang, An improved ATAC-seq protocol reduces background and enables interrogation of frozen tissues. *Nat. Methods* **14**, 959–962 (2017).
82. S. Andrews, FastQC: A Quality Control Tool for High Throughput Sequence Data [Online]. http://bioinformatics.babraham.ac.uk/projects/fastqc (2018).
83. A. M. Bolger, M. Lohse, B. Usadel, Trimmomatic: A flexible trimmer for Illumina sequence data. *Bioinformatics* **30**, 2114–2120 (2014).
84. D. Kim, B. Langmead, S. L. Salzberg, HISAT: A fast spliced aligner with low memory requirements. *Nat. Methods* **12**, 357–360 (2015).
85. D. R. Zerbino, P. Achuthan, W. Akanni, M. R. Amode, D. Barrell, J. Bhai, K. Billis, C. Cummins, A. Gall, C. G. Giron, L. Gil, L. Gordon, L. Haggerty, E. Haskell, T. Hourlier, O. G. Izuogu, S. H. Janacek, T. Juettemann, J. K. To, M. R. Laird, I. Lavidas, Z. Liu, J. E. Loveland, T. Maurel, W. McLaren, B. Moore, J. Mudge, D. N. Murphy, V. Newman, M. Nuhn, D. Ogeh, C. K. Ong, A. Parker, M. Patricio, H. S. Riat, H. Schuilenburg, D. Sheppard, H. Sparrow, K. Taylor, A. Thormann, A. Vullo, B. Walts, A. Zadissa, A. Frankish, S. E. Hunt, M. Kostadima, N. Langridge, F. J. Martin, M. Muffato, E. Perry, M. Ruffier, D. M. Staines, S. J. Trevanion, B. L. Aken, F. Cunningham, A. Yates, P. Flicek, Ensembl 2018. *Nucleic Acids Res.* **46**, D754–D761 (2018).
86. H. Li, B. Handsaker, A. Wysoker, T. Fennell, J. Ruan, N. Homer, G. Marth, G. Abecasis, R. Durbin; 1000 Genome Project Data Processing Subgroup, The Sequence Alignment/Map format and SAMtools. *Bioinformatics* **25**, 2078–2079 (2009).
87. Y. Liao, G. K. Smyth, W. Shi, FeatureCounts: An efficient general purpose program for assigning sequence reads to genomic features. *Bioinformatics* **30**, 923–930 (2014).
88. J. M. Gaspar, Genrich: Detecting sites of genomic enrichment. http://github.com/jsh58/Genrich (2019).
89. H. M. Amemiya, A. Kundaje, A. P. Boyle, The ENCODE blacklist: Identification of problematic regions of the genome. *Sci. Rep.* **9**, 9354 (2019).
90. A. R. Quinlan, N. Kindlon, Bedtools: A powerful toolset for genome arithmetic [Online]. https://bedtools.readthedocs.io/en/latest/ (2021).
91. F. Ramirez, D. P. Ryan, B. Gruning, V. Bhardwaj, F. Kilpert, A. S. Richter, S. Heyne, F. Dundar, T. Manke, DeepTools2: A next generation web server for deep-sequencing data analysis. *Nucleic Acids Res.* **44**, W160–W165 (2016).
92. J. T. Robinson, H. Thorvaldsdottir, W. Winckler, M. Guttman, E. S. Lander, G. Getz, J. P. Mesirov, Integrative genomics viewer. *Nat. Biotechnol.* **29**, 24–26 (2011).
93. S. Heinz, C. Benner, N. Spann, E. Bertolino, Y. C. Lin, P. Laslo, J. X. Cheng, C. Murre, H. Singh, C. K. Glass, Simple combinations of lineage-determining transcription factors prime cis-regulatory elements required for macrophage and B cell identities. *Mol. Cell* **38**, 576–589 (2010).
94. C. Benner, HOMER: Software for motif discovery and next generation sequencing analysis [Online]. http://homer.ucsd.edu/homer/ (2019).
95. M. I. Love, W. Huber, S. Anders, Moderated estimation of fold change and dispersion for RNA-seq data with DESeq2. *Genome Biol.* **15**, 550 (2014).
96. A. Zhu, J. G. Ibrahim, M. I. Love, Heavy-tailed prior distributions for sequence count data: Removing the noise and preserving large differences. *Bioinformatics* **35**, 2084–2092 (2019).
97. G. Yu, L.-G. Wang, Y. Han, Q.-Y. He, ClusterProfiler: An R package for comparing biological themes among gene clusters. *OMICS* **16**, 284–287 (2012).
98. D. Szklarczyk, A. L. Gable, D. Lyon, A. Junge, S. Wyder, J. Huerta-Cepas, M. Simonovic, N. T. Doncheva, J. H. Morris, P. Bork, L. J. Jensen, C. V. Mering, STRING v11: Protein-protein association networks with increased coverage, supporting functional discovery in genome-wide experimental datasets. *Nucleic Acids Res.* **47**, D607–D613 (2019).
99. A. Subramanian, P. Tamayo, V. K. Mootha, S. Mukherjee, B. L. Ebert, M. A. Gillette, A. Paulovich, S. L. Pomeroy, T. R. Golub, E. S. Lander, J. P. Mesirov, Gene set enrichment analysis: A knowledge-based approach for interpreting genome-wide expression profiles. *Proc. Natl. Acad. Sci. U.S.A.* **102**, 15545–15550 (2005).

Acknowledgments: We thank Hou laboratory and Zhu laboratory members for project assistance. **Funding:** This work was supported by the National Key Research and Development Program of China (2019YFA0508900 and 2021YFC2300501), the Chinese Academy of Sciences (XDB29050600 and XDB37010100), the National Natural Science Foundation of China (81991495, 31900467, 32100713, and 32288102), and the K. C. Wong Educational Foundation (GJTD-2020-06). B.Z. is supported by the New Cornerstone Investigator Program. **Author contributions:** X.Zhu and S.H. performed the majority of experiments. J.B., S.H., and Z.H. analyzed the sequencing data. Y.L., C.L., R.L., T.Z., Z.Z., L.L., and X.Zhou assisted the experiments. B.Z. and B.H. designed and supervised the study. Z.H., B.Z., and B.H. wrote the manuscript. **Competing interests:** The authors declare that they have no competing interests. **Data and materials availability:** All data needed to evaluate the conclusions in the paper are present in the paper and/or the Supplementary Materials. RNA-seq and ATAC-seq datasets have been deposited in the National Genomics Data Center (NGDC) under accession ID: CRA004767 and publicly accessible at https://ngdc.cncb.ac.cn/gsa.

Submitted 1 August 2023
Accepted 26 February 2024
Published 29 March 2024
10.1126/sciadv.adk0858